K888A, K907A, and K909A. The mutant *rig-I* genes were made by PCR-mediated site-directed mutagenesis. The primers used for the PCR were as follows: K907–909A-forward, GTT CAG ACA CTG TAC TCG GCG TGG GCG GAC TTT CAT TTT GAG AAG, and K907–909A-reverse, CTT CTC AAA ATG AAA GTC CGC CCA CGC CGA GTA CAG TGT CTG AAC; K888A-forward, GAC ATT TGA GAT TCC AGT TAT AGC AAT TGA AAG TTT TGT GGT GGA GG, and K888A-reverse, CCT CCA CCA CAA AAC TTT CAA TTG CTA TAA CTG GAA TCT CAA ATG TC; K849–851A-forward, GAG TAG ACC ACA TCC CGC CCA GCG CAG TTT TCA AGT TTT G, and K849–851A-reverse, CAA AAC TTG AAA ACT GCG CTG GCG CGG GAT GTG GTC TAC TC. PCR was carried with Pyrobest *Taq* polymerase, and the obtained clones were sequenced to exclude the clones harboring PCR error. To construct the plasmid-expressing mutant RIG-I protein, the wild-type *RIG-I* gene on pEF-BOS vector was replaced with the mutant *rig-I* gene.

Real Time PCR—Quantitative PCR analyses were carried out using iCycler iQ real time detection system with Platinum SYBR Green qPCR SuperMix-UDG reagent (Invitrogen). Primer sequences for qPCR were as follows: hGAPDH-qF, GAG TCA ACG GAT TTG GTC GT, and hGAPDH-qR, TTG ATT TTG GAG GGA TCT CG; hIFN- -qF, TGG GAG GAT TCT GCA TTA CC, and hIFN- -qR, CAG CAT CTG CTG GTT GAA GA; hMx1-qF, ACC ACA GAG GCT CTC AGC AT, and hMx1-qR, CTC AGC TGG TCC TGG ATC TC; and hIFIT-1-qF, GCA GCC AAG TTT TAC CGA AG, and hIFIT-1-qR, CAC CTC AAA TGT GGG CTT TT. Values were expressed as mean relative stimulations, and for a representative experiment from a minimum of three separate experiments, each was performed in triplicate.

RESULTS

RIG-I-binding Proteins—To isolate the proteins that bind to RIG-I, we performed yeast two-hybrid screening using a human lung cDNA library. Using the RIG-I central region (213–601 amino acids), we isolated a clone that encoded a partial ORF of a gene expressed in a dendritic cell line, DC12, whereas the C-terminal region of RIG-I (557–925 amino acids) resulted in the isolation of two cDNA clones, which encoded partial C-terminal regions of ZNF598 and RNF135 (Fig. 1*A* and data not shown). Preliminary expression studies showed that the RNF135 segment affected the RIG-I IFN- inducing activity, whereas the other two proteins had no effect (data not shown). We confirmed the

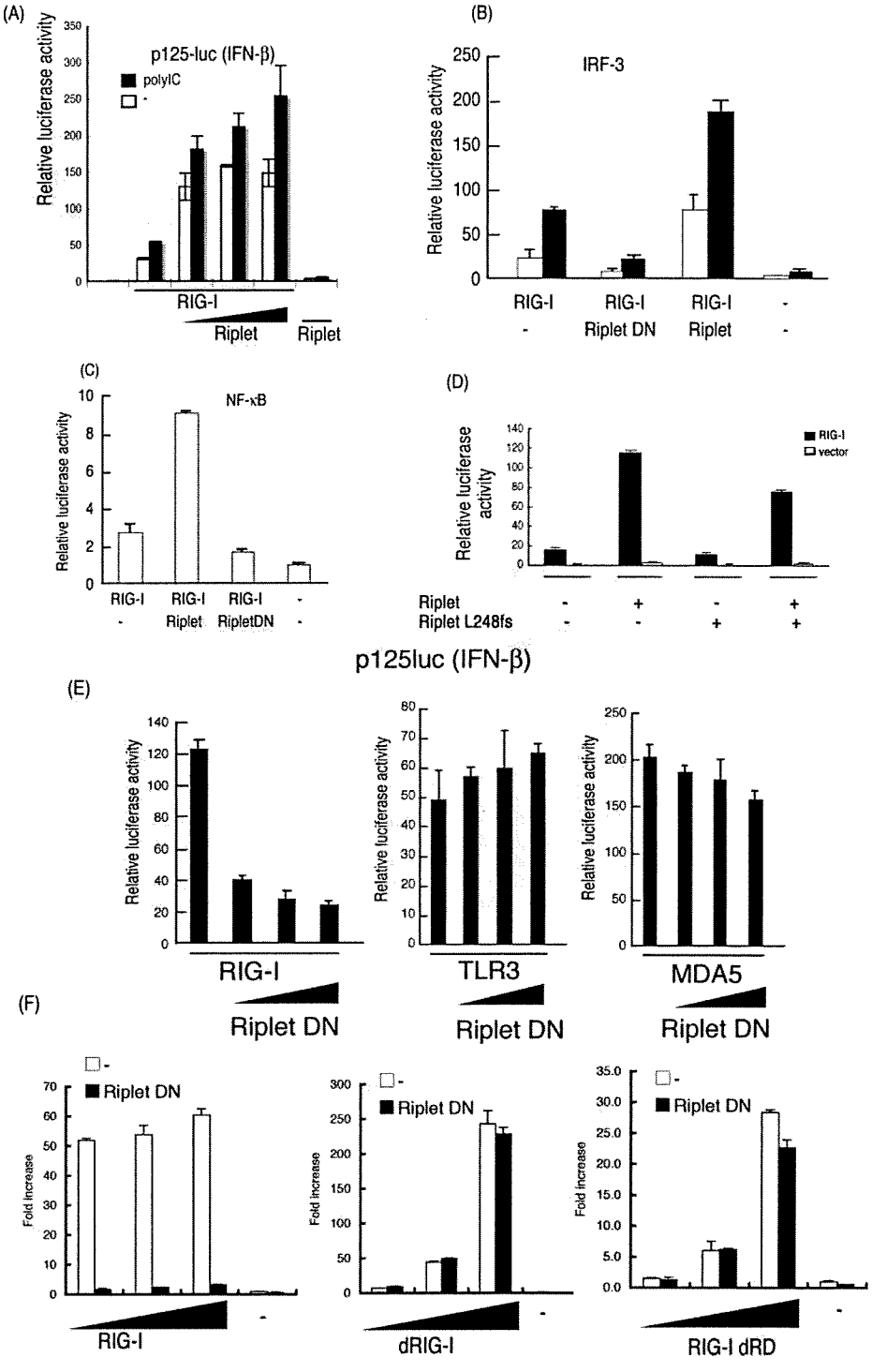

interaction of RIG-I with ZNF598 or RNF135 in HEK293FT cells by immunoprecipitation (data not shown). RNF135 was previously annotated by the genome project and was recently found to be a cause of a genetic disease, neurofibromatosis, although its protein function was unknown. We renamed the protein Riplet (RING finger protein leading to RIG-I activation) based on the following functional analyses. Riplet was most similar to TRIM25 (60.8% sequence homology), in particular between their RING finger domains PRY or SPRY (Fig. 1*B*). Phylogenetic analysis also supported the notion that Riplet was similar to TRIM25 (Fig. 1*C*). Thus, we hypothesized that, like TRIM25, Riplet is a ubiquitin ligase.

Expression of Riplet—RIG-I mRNA is induced by type I IFN or poly(I-C) stimulation in mammalian cells. Unlike RIG-I, however, Riplet mRNA was basally expressed in HeLa and primary-cultured MRC-5 cells irrespective of stimulation (Fig. 1*D* and data not shown). On the other hand, when we treated bone marrow-derived dendritic cells with poly(I-C), the basal level of Riplet mRNA was increased by the stimulation (Fig. 1*D*), suggesting that the regulatory mechanism of Riplet expression somewhat differs among cell types, and that Riplet is expressed before virus infection in some cell types. Next we performed Northern blotting of human tissue RNA. Riplet mRNA was detected as a single band of 2.4 kbp, which is slightly longer than the RNF135 cDNA sequence deposited in GenBank™ (accession number AB470605). Human *RIPLET* is expressed in human skeletal muscle, spleen, kidney, placenta, prostate, stomach, thyroid, and tongue and also weakly expressed in heart thymus, liver, and lung (Fig. 1*E*).

Riplet Enhances RIG-I-mediated IFN- Induction—At first we characterized the role of Riplet in RIG-I-mediated IFN inducing signaling by reporter gene analyses. When RIG-I was expressed in HEK293 cells, reporter auto-activation was observed even in the absence of exogenous stimulation (Fig. 2*A*) as reported previously (25, 26). Stimulation with poly(I-C) further enhanced the promoter. Co-expression of Riplet with RIG-I potentiated activation of the IFN- promoter, whereas expression of Riplet alone resulted in only marginal activation (Fig. 2*A*). Detection of endogenous IFN- mRNA confirmed that Riplet enhanced RIG-I-mediated activation of IFN- transcription (supplemental Fig. S1). The enhancing role of Riplet in IFN- promoter activation was also supported by activation of IRF-3 and NF- B by Riplet (Fig. 2, *B* and *C*). In contrast, expression of a Riplet partial fragment (Riplet-DN) (70–432 amino acids) that lacked the N-terminal RING finger domain reduced promoter activation (Fig. 2*E*). The Riplet-L249fs mutant protein, which was isolated from neurofibromatosis patients (27), did not increase the RIG-I-mediated promoter activation (Fig. 2*D*). These data indicate that Riplet augments RIG-I-mediated IFN- promoter activation, and that both the RING finger domain and the C-terminal region encoding the SPRY and PRY motifs are important for its function. Riplet (residues 70–432) acted as a dominant-negative form (hereafter called Riplet-DN) (Fig. 2, *E* and *F, left panel*). This functional feature of Riplet-DN was confirmed in Fig. 2, *B* and *C*, and was later confirmed through RIG-I co-precipitation and ubiquitination analyses (see Fig. 5*C* and supplemental Fig. S4*C*). Expression of Riplet-DN did not reduce TLR3 or MDA5 signaling (Fig. 2*E*), suggesting that Riplet-DN is specific for RIG-I signaling. Interestingly, the Riplet-DN only partially suppressed the function of the C-terminal deleted RIG-I (dRD), which is a constitutively active form (Fig. 2*F, right panel*), and RIG-I CARD-like region (dRIG-I)-mediated signaling in high or low dose transfection of dRIG-I was barely inhibited by overexpression of Riplet-DN (Fig. 2*F, center panel*). These data suggest that Riplet requires the RIG-I C-terminal domain (RD) and partial helicase region to activate RIG-I signaling.

Endogenous Riplet Promotes the RIG-I Signaling—We performed Riplet knockdown by siRNA Riplet using Lipofectamine 2000 reagents, instead of FuGENE HD, to reveal the function of endogenous Riplet. Two siRNAs (Riplet siRNA and Riplet si-1) that target different sites of the Riplet mRNA and two control siRNAs were used for knockdown analyses. The two siRNA or control siRNA were co-transfected with HA-tagged Riplet expression vector into HEK293 cells, and after 48 h, cell lysate was prepared and analyzed by Western blotting with anti-HA antibody detecting Riplet. The two siRNAs targeting Riplet abolished exogenously expressed Ripelt-HA, but control siRNA did not (supplemental Fig. S3). Likewise, both Riplet siRNA and Riplet si-1 specifically down-regulate the level of endogenous Riplet mRNA (Fig. 3, *A* and *B*).

Using the siRNA, we examined whether Riplet knockdown reduces RIG-I signaling. As expected, RIG-I-mediated IFN- promoter activation was reduced by Riplet siRNA or Riplet si-1 compared with control siRNA (Fig. 3, *A* and *B*), indicating that Riplet is required for full activation of the RIG-I signaling. Vesicular stomatitis virus (VSV) is a negative-stranded RNA virus that induces IFN- production via RIG-I (3). Although the

FIGURE 2. Riplet enhances IFN- signaling mediated by RIG-I. A, Riplet enhances the promoter activation by RIG-I. HEK293 cells were transfected with plasmids encoding empty vector, RIG-I (0.1 g) and Riplet (0.025, 0.05, or 0.1 g) together with p125-luc (IFN- promoter) reporter plasmid in 24-well plates. 24 h after transfection, the cells were treated with mock or poly(I-C) (50 g/ml) for 4 h as described under "Experimental Procedures," and then luciferase activities of cell lysates were measured. Closed or open boxes represent poly(I-C) or mock stimulation, respectively. B, to examine the activation of IRF-3, RIG-I (0.1 g), Riplet (0.1 g), and/or Riplet-DN (0.1 g),expressing vectors were transfected into HEK293 cells with reporter plasmids, GAL4 fused IRF-3 (0.05 g), and the p55 UASG-luc reporter gene (0.05 g), in which luciferase reporter gene is fused downstream of GAL4 protein-binding site, and therefore activated IRF-3 promotes the transcription of luciferase reporter gene. The cells were stimulated with poly(I-C) as described above (34). The total amount of transfected DNA (0.5 g/well) was kept constant by adding empty vector (pEF-BOS). C, HEK293 cells were transfected with RIG-I (0.1 g), Riplet (0.1 g), and/or Riplet-DN (0.1 g) expressing vectors together with the NF- B reporter plasmid (0.1 g), and 24 h later, the luciferase activities of cell lysates were measured. D, Riplet-L248fs, which lacks the C-terminal region, did not enhance the activation at all. HEK293 cells were transfected with the plasmids expressing wild-type Riplet (0.1 g) or Riplet-L248fs (0.1 g) together with RIG-I expressing vector (0.1 g) and p125-luc reporter (0.1 g). 24 h after transfection, cell were stimulated with poly(I-C), and the luciferase activities of cell lysates were determined as described above. E, RIG-I (0.1 g), MDA5 (0.1 g), or TLR3 (0.1 g) expressing vectors were transfected into HEK293 cells with the plasmid encoding the Riplet-DN fragment (0.1, 0.2, or 0.3 g) in 24-well plates. After 24 h, the cells were stimulated with 50 g of poly(I-C) for 4 h, and relative luciferase activities were determined. F, Riplet-DN (100 ng) was co-transfected with full-length RIG-I (0, 50, 100, or 200 ng), RIG-I CARD-like region (dRIG-I) (0, 50, 100, or 200 ng), or C-terminal deleted RIG-I (RIG-I dRD) (0, 50, 100, or 200 ng) into HEK293 cells in 24-well plate, and reporter gene assays were carried out.

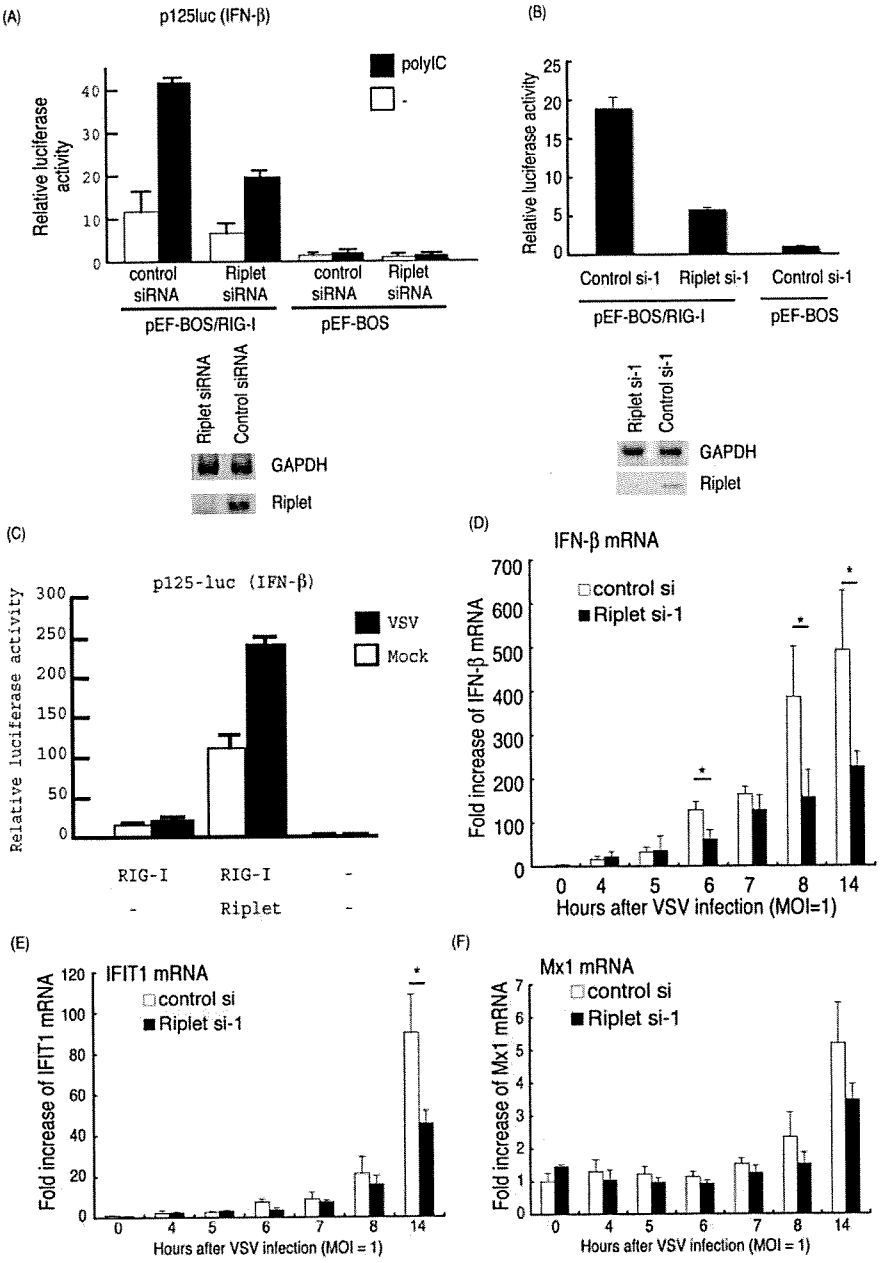

FIGURE 3. Knockdown analyses of Riplet. A, p125 luc reporter plasmid (0.1 g), RIG-I expressing vector (0.1 g), and Riplet siRNA or control siRNA (10 pmol), which were purchased from Funakoshi Co. Ltd., were transfected into HEK293 cells in a 24-well plate with Lipofectamine 2000, and 48 h after transfection, the cells were stimulated with poly(I-C) for 6 h, and the cell lysate was prepared, and luciferase activities were measured. RT-PCR was carried out using total RNA extracted from cells 48 h after transfection. B, p125 luc reporter plasmid (0.1 g), RIG-I expressing vector (0.1 g), and siRNA, Riplet si-1, or control si-1 (10 pmol), which were purchased from Applied Biosystems, were transfected into HEK293 cells with Lipofectamine 2000. 48 h after transfection, the cells were stimulated with poly(I-C) for 6 h. The cell lysate was prepared, and luciferase activities were measured. RT-PCR was carried out using total RNA extracted from cells 48 h after transfection. C, HEK293 cells were transfected with the plasmids expressing RIG-I (0.1 g) and/or Riplet (0.1 g) with p125 luc reporter plasmid (0.1 g) in 24-well plates. After 24 h, the cells were infected with VSV (m.o.i. 1) for 12 h. The luciferase activities of the cell lysates were measured. Expression of Riplet strongly enhanced IFN- promoter activation by VSV through RIG-I. D–F, siRNA (control si- or Riplet si-1) were transfected into HEK293 cells, and after 48 h, the cells were infected with VSV at m.o.i. 1. RNA was extracted at the indicated hours, and the quantitative PCR were carried out to detect the expression of IFN- (D), IFIT-1 (E), or Mx1 (F) mRNA. *, p 0.05. GAPDH, glyceraldehyde-3-phosphate dehydrogenase.

IFN- promoter was only minimally activated by RIG-I in response to VSV (m.o.i. 1) during the early phase of infection (12 h), the activity was increased by RIG-I and Riplet (Fig. 3*C*). Riplet was silenced by siRNA and then VSV infected the cells. VSV-derived up-regulation of IFN- mRNA was started around 6 h post-infection, and Riplet siRNA significantly suppressed the increase of IFN- mRNA at 6 h (Fig. 3*D*). Because VSV infection is mainly sensed by RIG-I, this is consistent with the notion that Riplet promotes the RIG-I signaling. Other IFN-inducible genes, *IFIT1* and *MX1*, were expressed 8 h post-infection, and their expressions were also suppressed by Riplet siRNA (Fig. 3, *E* and *F*).

Riplet Exerts Protective Activity against Viral Infection—Next we examined the role of Riplet during viral infection. Riplet and/or RIG-I were transiently expressed in the human cells by FuGENE HD reagents, and then the cells were infected with VSV or poliovirus (a positive-stranded RNA virus). The viral titer of the supernatant was determined 24 h post-infection. Under our conditions, expression of RIG-I weakly inhibited VSV propagation. Co-expression of Riplet with RIG-I significantly suppressed VSV replication especially at low m.o.i., whereas Riplet alone did not suppress VSV (Fig. 4, *A* and *B, upper panel*). Therefore, a sufficient amount of RIG-I protein is required for Riplet to exert antivirus activity. This requirement of RIG-I is also observed in reporter gene analyses (Fig. 2). Under a similar setting, the antiviral effect of Riplet was marginally observed against poliovirus, which induces IFN- largely via MDA5 (Fig. 4*B*, *lower panel*). To assess the importance of endogenous Riplet for antivirus effect of human cells, Riplet knockdown cells were infected with viruses. In Riplet knockdown cells, the VSV titer was consistently increased compared with the control (p 0.05) (Fig. 4*C*, *left panel*). In addition, infection of Riplet knockdown cells with poliovirus resulted in only a slight increase in the poliovirus titer compared with the control (p 0.05) (Fig. 4*C*, *right panel*). Because poliovirus is mainly recognized by MDA5 but not RIG-I, this marginal effect of Riplet on poliovirus infection was within expectation (3, 28).

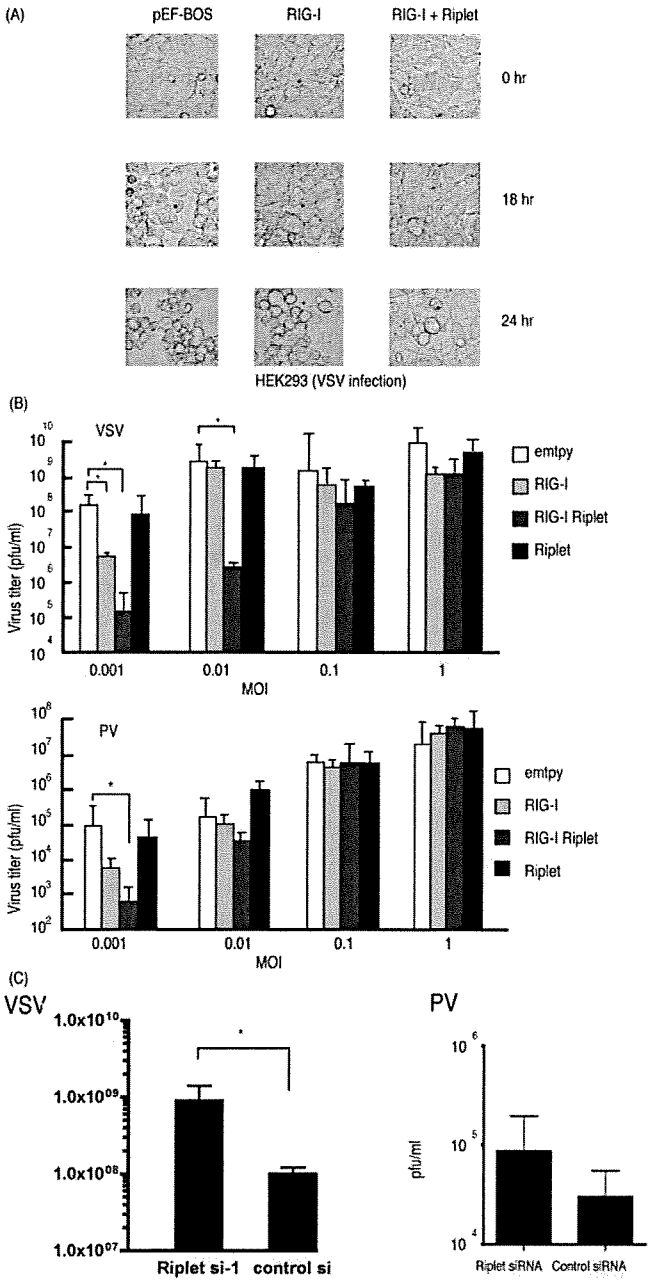

FIGURE 4. Suppression of RNA viruses by Riplet. A, HEK293 cells were transfected with RIG-I (0.1 g) and/or Riplet (0.1 g) expressing vectors. The total amount of transfected DNA (0.5 g/well) in each well was kept constant by adding empty vector (pEF-BOS). 24 h after transfection, the cells were infected with VSV at m.o.i. 0.1, and after 0, 18, or 24 h, CPE was observed by microscope. B, RIG-I (0.1 g) and/or Riplet (0.1 g) expressing plasmids were transfected to HEK293 cells in 24-well plates and incubated for 24 h. The total amount of transfected DNA (0.5 g/well) in each well was kept constant by adding empty vector (pEF-BOS). The cells were infected with VSV (upper panel) or poliovirus (PV) (lower panel) at the indicated m.o.i. The viral titers in the culture media were measured 24 h after infection by plaque assay. Error bars represent standard deviation (n 3). *, p 0.05. C, control or Riplet knockdown HEK293 cells were infected with VSV (left panel) or poliovirus (right panel) at m.o.i. 0.1. The viral titers in the culture media were measured 26 h after infection by plaque assays. Knockdown of Riplet induced higher VSV titers compared with control (p 0.05), but the increase observed in poliovirus-infected Riplet knockdown cells was not significant (p 0.05).

Riplet and Riplet-DN Bind the Helicase and RD Regions of RIG-I—Yeast two-hybrid analysis showed that a C-terminal region of Riplet bound to the C-terminal region of RIG-I. This cytoplasmic interaction between Riplet and RIG-I was confirmed by confocal microscopy in HeLa cells (supplemental Fig. S2). To further confirm the physical binding of Riplet to RIG-I in human cells, we carried out immunoprecipitation analyses. Full-length Riplet was co-immunoprecipitated with RIG-I (Fig. 5*B*), indicating that Riplet binds directly to RIG-I in human cells.

To determine the region responsible for the RIG-I-Riplet interaction, we constructed a RIG-I and Riplet deletion series as shown in Fig. 5*A*. Riplet-DN also bound to RIG-I (Fig. 5, *B* and *C*), indicating that the RING finger domain is dispensable for the RIG-I-Riplet interaction. This is consistent with the notion that the RING finger domain in ubiquitin ligase proteins is required for their interactions with ubiquitin-conjugating enzymes (29). Unlike TRIM25, Riplet and Riplet-DN failed to co-precipitate the two CARD domains of RIG-I (dRIG-I) (Fig. 5*D*). However, co-precipitation of the RIG-IC or RIG-RD fragments was observed (Fig. 5, *E* and *F*). RD-deleted RIG-I (RIG-I dRD) weakly associated with Riplet (Fig. 5*G*). Taken together, Riplet preferentially binds the RD and also weakly associates with the helicase region of RIG-I with its C terminus. Reporter gene analyses show that Riplet-DN only weakly suppresses RIG-I signaling and barely suppresses dRIG-I, which contains neither helicase nor RD region. Therefore, the physical interaction is correlated with the results of reporter activity.

Riplet Promotes Ubiquitination of RIG-I—Because Riplet shares 60% sequence similarity with TRIM25, we hypothesized that Riplet ubiquitinates RIG-I and that this modification leads to activation of RIG-I signaling. To test this hypothesis, we examined RIG-I ubiquitination. As expected, ubiquitination of RIG-I was increased by co-expression of Riplet under two different conditions (Fig. 6, *A* and *B*). The quantity of RIG-I ubiquitination was significantly high in the presence of Riplet (Fig. 6*C*). RIG-I ubiquitination was suppressed if Riplet was replaced with Riplet-DN (Fig. 6*D* and supplemental Fig. S4*C*). However, unlike TRIM25, Riplet binds to the C-terminal region of RIG-I. Therefore, we examined whether Riplet ubiquitinates the C-terminal region. We found that ubiquitination of RIG-IC was enhanced by Riplet expression (Fig. 6*E*). Both RIG-I dRD and RIG-I RD were also ubiquitinated by expression of Riplet (Fig. 6*F*; supplemental Fig. S4*A* and S5), suggesting that Riplet promotes ubiquitination of the helicase and RD domains of RIG-I in a manner distinct from TRIM25.

Ubiquitin is polymerized through its lysine residue. Lys-63-linked polyubiquitination is frequently observed in signal transduction pathways (30). In contrast, Lys-48-linked polyubiquitination usually leads to the degradation of protein through the proteasome. Indeed, TRIM25-mediated Lys-63-linked polyubiquitination activates the CARD-like region of RIG-I, and RNF125-mediated Lys-48-linked polyubiquitination leads to the degradation of RIG-I (23, 25). We used K48R or K63R mutated ubiquitin and found that K48R was incorporated normally into RIG-IC, whereas polyubiquitination was decreased by K63R (supplemental Fig. S4*B*). K63R mutation abolished RIG-I RD polyubiquitination by Riplet (Fig. 6*F*). These data

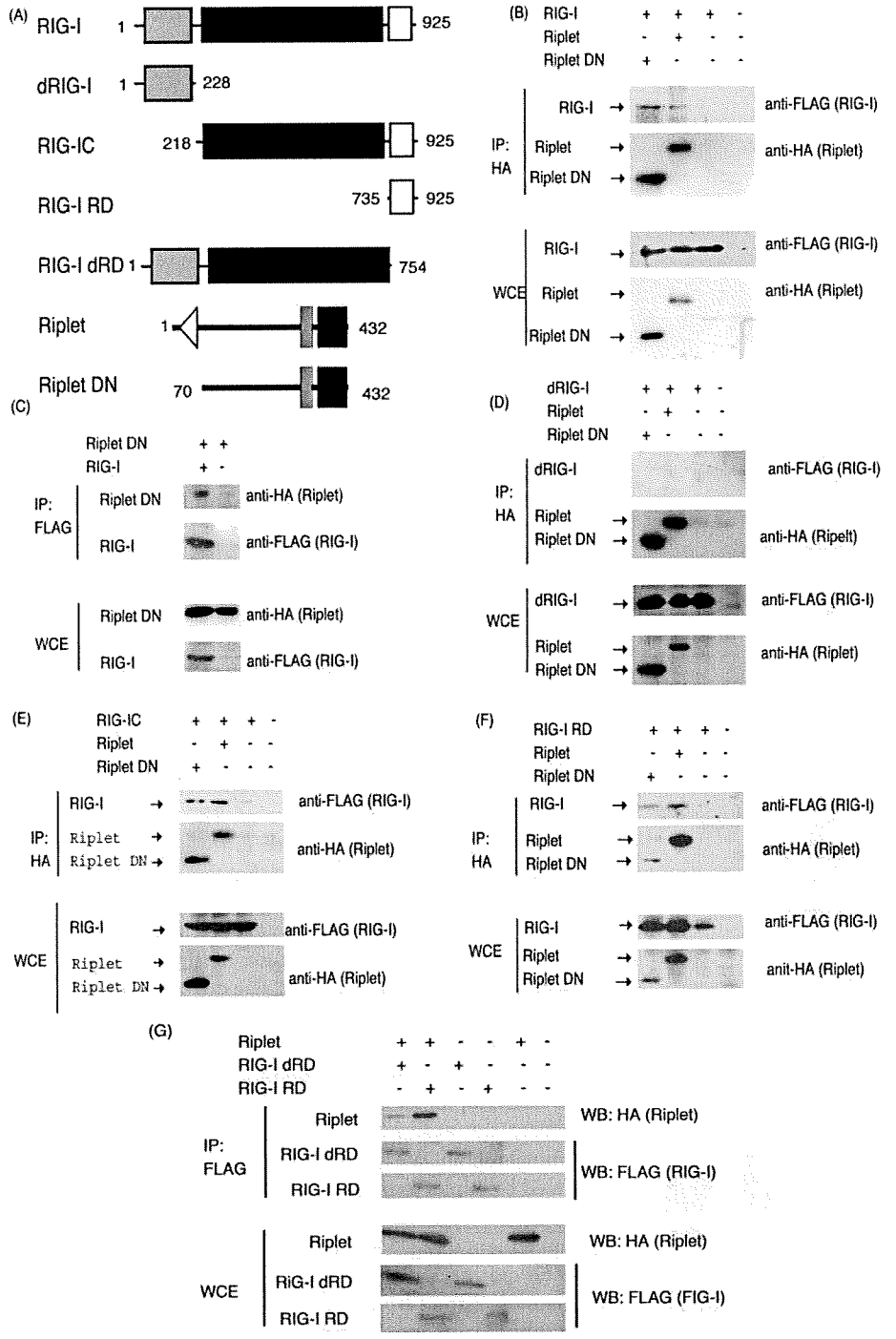

FIGURE 5. Physical interaction of Riplet with RIG-I. A, schematic representation of RIG-I or Riplet fragments used for immunoprecipitation analyses. B, HA-tagged Riplet (0.4 g) or Riplet-DN (0.4 g) were transfected into HEK293FT cells in a 6-well plate with FLAG-tagged RIG-I (0.4 g). HA-tagged Riplet or Riplet-DN were immunoprecipitated (IP) with anti-HA antibodies, and samples were analyzed by Western blotting (WB) using an anti-FLAG or anti-HA antibody. The total amount of transfected DNA (2 g/well) was kept constant by adding empty vector (pEF-BOS). C, HA-tagged Riplet-DN (0.4 g) and FLAG-tagged RIG-I (0.4 g) were transfected into HEK293FT cells in a 6-well plate. RIG-I was immunoprecipitated with anti-FLAG antibody, and samples were analyzed by Western blotting using an anti-FLAG or -HA antibody. The total amount of transfected DNA (2 g/well) was kept constant by adding empty vector (pEF-BOS). D–F, interaction of HA-tagged Riplet or Riplet-DN with FLAG-tagged dRIG-I (D), RIG-IC (E), or RIG-I RD (F) was examined using immunoprecipitation assays. The proteins were expressed in HEK293FT cells, and HA-tagged Riplet was immunoprecipitated with anti-HA antibody, and samples were analyzed by Western blotting using an anti-FLAG or -HA antibody. G, FLAG-tagged RIG-I RD (0.4 g) or RIG-I dRD (0.4 g) was transfected with HA-tagged Riplet (0.4 g) into HEK293 FT cells in a 6-well plate, and 24 h after transfection, immunoprecipitation was performed with anti-FLAG antibody and analyzed by Western blotting. The total amount of transfected DNA (2 g/well) was kept constant by adding empty vector (pEF-BOS). WCE, whole cell extract.

indicates that Riplet mediates Lys-63-linked polyubiquitination of the RIG-I C-terminal helicase and RD region. Because Riplet-DN reduced the RIG-I-mediated signaling, we examined whether Riplet-DN reduced the RIG-I ubiquitination. As expected, Riplet-DN reduced RIG-I ubiquitination (Fig. 6*D* and supplemental Fig. S4*C*). These ubiquitination assay data are consistent with the notion that Riplet-mediated Lys-63-linked polyubiquitination of RIG-I is required for full activation of RIG-I signaling.

We tried to determine the ubiquitination sites of RIG-I using Lys-to-Ala (KA)-converting mutants. RIG-I has 25 Lys residues in its C-terminal region. These Lys residues of RIG-I were in turn mutated to Ala, and the degree of ubiquitination and IFN- -inducing activity were determined with each mutant. RIG-I-mediated IFN- promoter activation was normally augmented by co-expression of Riplet and 3KA RIG-I. Co-expression of Riplet and 5KA, however, and the ubiquitination level of RIG-I and IFN- -inducing activity were simultaneously decreased (Fig. 7, *A* and *C*). Riplet-dependent augmentation of IFN- promoter activation was largely suppressed when RIG-I was replaced with 5KA RIG-I (Fig. 7*B*). Therefore, Lys-849 and Lys-851 of RIG-I were crucial for RIG-I ubiquitination by Riplet. The results confirmed the importance of ubiquitination of specific Lys residues in the C-terminal region of RIG-I and for RIG-I-mediated IFN- induction.

DISCUSSION

RIG-I plays a central role in the recognition of cytoplasmic viral RNA and is regulated by modification by small modifier ubiquitin or ubiquitin-like protein, ISG15. TRIM25 mediates Lys-63-linked polyubiquitination, which is essential for RIG-I activation (23), and RNF125 mediates Lys-48-linked polyubiquitination (25). RIG-I also harbors ISG15 modification, although the role of ISG15 modification *in vivo* remains to be deter-

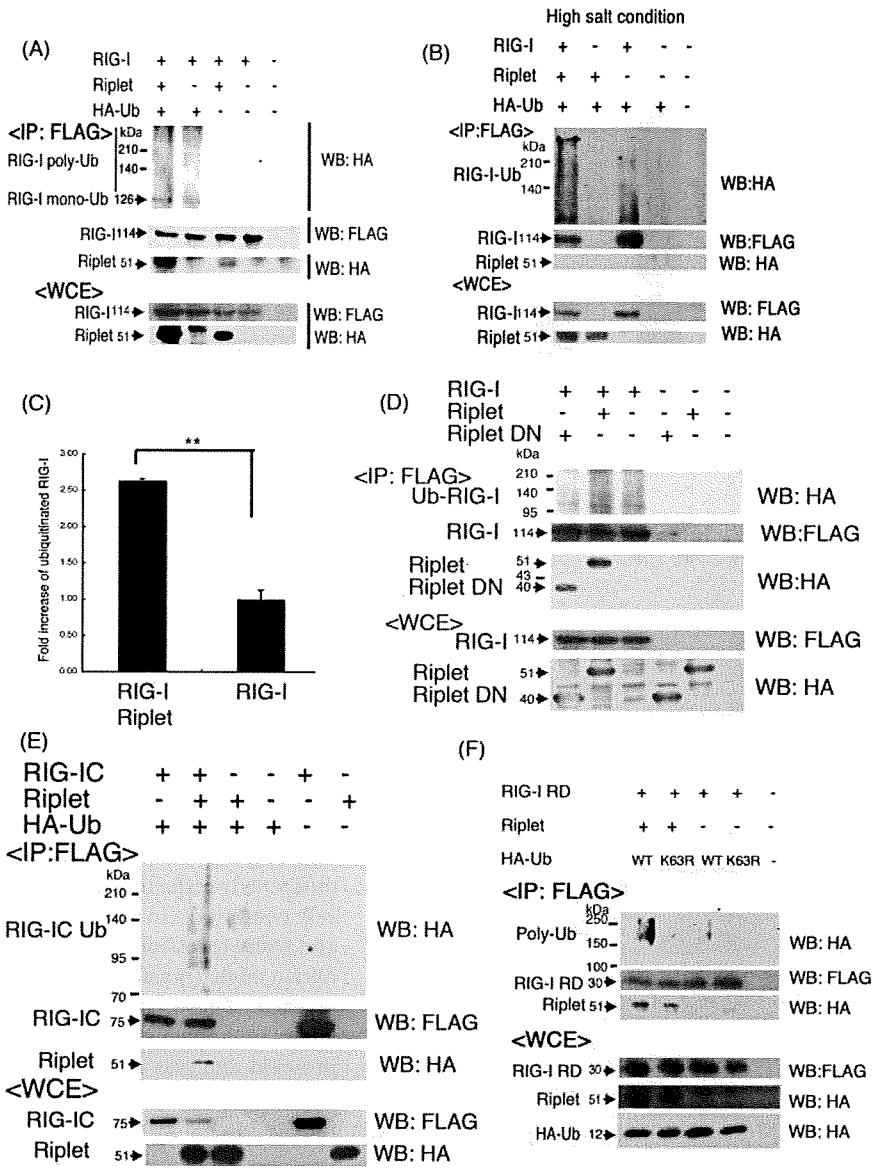

FIGURE 6. Ubiquitination of RIG-I by Riplet. A and B, FLAG-tagged RIG-I (0.4 g), Riplet (0.4 g), and HA-tagged ubiquitin (0.4 g) expressing vectors were transfected into HEK293FT cells in 6-well plates. The total amount of transfected DNA (2 g/well) was kept constant by adding empty vector (pEF-BOS). FLAG-tagged RIG-I was immunoprecipitated (IP) using an anti-FLAG antibody, and washed with the buffer containing 150 mM NaCl (A) or 1 M NaCl (B). The immunoprecipitates were separated with 8% acrylamide gel and analyzed by Western blotting (WB) using antibodies against HA tag (ubiquitin) or FLAG (RIG-I). Riplet was co-immunoprecipitated with FLAG-tagged RIG-I in A but could not co-immunoprecipitate in B because of high salt condition. Expression of Riplet enhanced the ubiquitination of RIG-I. Different gel conditions were employed in A and B. C, ubiquitinated RIG-I was quantitated with NIH image software. **, p 0.01. D, FLAG-tagged RIG-I (0.4 g) was transfected into HEK293 FT cells in a 6-well plate with HA-tagged Riplet (0.4 g) or Riplet-DN (0.4 g) and HA-tagged ubiquitin, and immunoprecipitation was carried out with anti-FLAG antibody. The total amount of transfected DNA (2 g/well) was kept constant by adding empty vector (pEF-BOS). The samples were analyzed with 10% acrylamide gel to clearly separate Riplet from Riplet-DN and stained by Western blotting. E, ubiquitination of RIG-IC was also promoted by Riplet expression. HEK293FT cells were transfected with the plasmids encoding RIG-IC (0.4 g), Riplet (0.4 g), and/or HA-tagged ubiquitin (0.4 g) in a 6-well plate, and 24 h after transfection, cell lysates were prepared. The total amount of transfected DNA (2 g/well) was kept constant by adding empty vector (pEF-BOS). FLAG-tagged RIG-ICs were immunoprecipitated with anti-FLAG antibodies, and the proteins were analyzed by Western blotting. F, Ub-K63R are HA-tagged ubiquitin in which the lysine 3 residues were substituted with arginine. The HA-tagged Ub-K63 expressing vectors (1.2 g), FLAG-tagged RIG-IC (0.4 g), and/or Riplet (0.4 g) were transfected into HEK293FT cells in 6-well plates and analyzed as shown in A–D. The total amount of transfected DNA (2 g/well) was kept constant by adding empty vector (pEF-BOS). Ub-K63R was not incorporated into polyubiquitin chain of RIG-I RD. WCE, whole cell extract.

mined (21, 22, 31). Although Riplet and TRIM25 share 60% sequence similarity, the ubiquitination of RIG-I by Riplet is distinct from that by TRIM25; Riplet ubiquitinates the C-terminal region of RIG-I, whereas TRIM25 ubiquitinates its CARD-like region. These findings are also supported by the fact that neither Riplet nor Riplet-DN promoted or inhibited the activation of the IFN- promoter by expression of the RIG-I CARD-like region (data not shown). It has been reported that ubiquitination of the CARD-like region of RIG-I by TRIM25 is critical for RIG-I-IPS-1 signaling (23). However, how this CARD ubiquitination is essential for activation of IPS-1 by RIG-I remains undetermined. Here we emphasize the importance of RIG-I C-terminal ubiquitination for IFN- induction and the antiviral response. Because the C-terminal RD region inhibits the IFN inducing activity of the CARD-like region of RIG-I, it is reasonable that RIG-I C-terminal ubiquitination by Riplet inhibits the conversion from the active to inactive form of RIG-I protein after binding to viral RNA. This initial stabilization of RIG-I via ubiquitination by Riplet would provide a sufficient structure for RIG-I to maintain the accessibility to TRIM25 and facilitate TRIM25-mediated ubiquitination of the CARD-like region of RIG-I, which may lead to potential activation of IPS-1.

RIG-I is an IFN-inducible RNA helicase that is expressed at extremely low levels in resting cells (6). Initial penetration of viruses allows generation of 5 -triphosphate RNA and/or double strand RNA followed by induction of IFN- production. This early response to viral infections triggers up-regulation of RIG-I/MDA5 and TLR3, leading to robust IFN- production (3, 32, 33). We favor the interpretation of our present findings that during the early stages of viral infection with trace amounts of RIG-I and viral RNAs, Riplet helps host cells rearrange RIG-I conformation to activate IPS-1. This issue will need further proof because it is difficult to

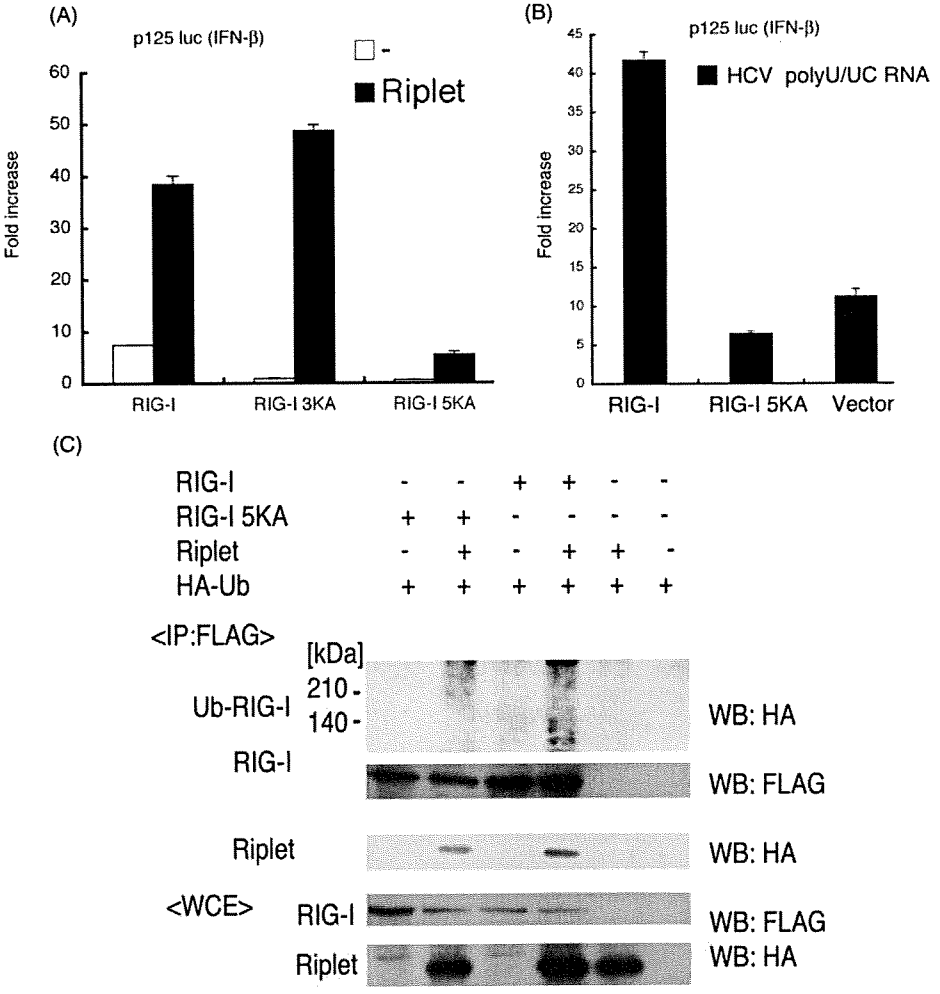

FIGURE 7. The C-terminal two lysine residues of RIG-I are important for ubiquitination by Riplet. A, RIG-I C-terminal lysine residues were substituted with alanine. RIG-I 3KA mutant protein harbors the triple mutations, K888A, K907A, and K909A. The five lysine residues, Lys-849, Lys-851, Lys-888, Lys-907, and Lys-909, were replaced with alanine in RIG-I 5KA mutant. The plasmid carrying wild-type (100 ng/well), RIG-I 3KA (100 ng/well), RIG-I 5KA (100 ng), or Riplet (100 ng) were transfected into HEK293 cells in a 24-well plate together with p125 luc reporter plasmid (100 ng/well). The amount of transfected DNA was kept constant by adding empty vector. After 24 h, the luciferase activities were measured. B, wild-type RIG-I (100 ng), RIG-I 5KA mutant (100 ng), or empty vector (100 ng) was transfected into HEK293 cells in a 24-well plate together with p125 luc reporter plasmids and HCV 3 -untranslated region poly(U/UC) RNA (25 ng), which is synthesized in in vitro transcription by T7 RNA polymerase. The amount of transfected DNA was kept constant by adding empty vector. 24 h after transfection, luciferase activities were measured. RIG-I 5KA mutant hardly responded to poly(U/UC) RNA. C, to observe the ubiquitinated RIG-I more clearly, we used 800 ng/well of Riplet and HA-Ub expression vector for the following transfection. HEK293FT cells in a 6-well plate were transfected with the plasmids encoding RIG-I (400 ng/well), RIG-I 5KA (400 ng/well), Riplet (800 ng/well), and/or HA-Ub (800 ng/well). The total amount of DNA was kept constant by adding the empty vector. 24 h after the transfection, the cell lysates were prepared, and the immunoprecipitation was carried out using anti-FLAG antibodies. The immunoprecipitates were analyzed by Western blotting with anti-HA or FLAG antibodies.

visualize RNRs and viral RNAs in the early infection stage and to understand the mechanisms that allow viruses to uncoat into naked viral RNA and to replicate.

We have provided several lines of evidence indicating that Riplet complements RIG-I-mediated IFN- induction upon viral infection by both Riplet siRNA and overexpression analyses. The C-terminal lysines (849 and 851) of RIG-I are critical for Riplet-mediated RIG-I ubiquitination. However, our data indicate that Riplet alone was unable to induce IFN- production and essentially required RIG-I to confer IFN- induction. Furthermore, Riplet is not ubiquitously distributed over the organs tested. Ubiquitination of RIG-I induced by poly(I-C) or viruses was accelerated in cells pre-transfected with Riplet. Hence, Riplet works case-sensitive to up-regulate RIG-I antiviral activity predominantly in some organs. The physiological meaning of this response will be clarified by knock-out study.

Unexpectedly, the siRNA experiments were not robust with regard to VSV replication. Possible explanations for this are as follows: 1) the degree of gene silencing is not so profound that the proteins remain in the cells; 2) there are a number of virus-mediated IFN-inducing pathways capable of compensating each other, so that disruption of one factor does not cause a profound effect on VSV replication. Furthermore, in VSV-infected Riplet-knockdown cells, IFN- levels were reduced even at m.o.i. 1 (Fig. 3*D*), and accordingly, virus susceptibility was increased at m.o.i. 0.1 (Fig. 4*C*), whereas in Riplet-overexpressing cells, antiviral activity was observed only at low m.o.i. (Fig. 4*B*). We used different transfection reagents and cell conditions in the knockdown and overexpression experiments to obtain high transfection efficiency in each. These conditional differences in knockdown and overexpression analyses might cause part of the discrepancy between the two results on Riplet antiviral activity. Another possibility to explain the apparent inconsistencies between overexpression and knockdown analyses is that high amounts of Riplet efficiently activate the RIG-I signaling, but low amounts are insufficient for RIG-I activation in high m.o.i.-infecting human cells. High amounts of Riplet with overexpressed RIG-I would confer the ability on cells to respond to very low amounts of VSV as observed in the low m.o.i. experiments. Again, *riplet* knock-out mice would reveal whether it is absolutely required for potential RIG-I activation.

How viral RNAs select RIG-I rather than dicers or the translation machinery is also unknown. During natural infection it is likely that the number of the initial invading virions would be at most several copies/cell. Uncoated viral RNA may assemble a complex consisting of viral and host molecules required for replication. We assume that cells are equipped with various

molecular arms to sensitively detect viral RNA. The molecular complexes sensing viral RNA may not be so simple that we will be able to identify more molecules than Riplet as enhancers for integral RNA recognition. In either case, yeast screening will be a good strategy to pick up such proteins in other RNA recognition systems. A molecular switch selecting IFN induction by virus RNA will then be clarified.

We show that the ubiquitination sites targeted by Riplet are the helicase and RD domains of RIG-I but not its CARD-like domains in contrast to TRIM25. Riplet may be a complement factor of the reported TRIM25 function for RIG-I activation (23). A previous report (25) failed to polyubiquitinate the RIG-I protein by TRIM25 alone. If Riplet were added to TRIM25 for RIG-I ubiquitination in the previous study, Riplet would have enabled TRIM25 to polyubiquitinate the RIG-I CARD-like region. Further studies using TRIM25 and Riplet will be required to clarify this point.

Based on our results, we propose that RIG-I-like receptors form a molecular complex that efficiently recognizes low copy numbers of viral RNA. Riplet is implicated in the RIG-I complex to enhance viral RNA response in some organs. In this context, MDA5-associated molecules might also exist in the cytoplasm to augment IFN output. Although MDA5 possesses the RD domain, it fails to recruit Riplet (data not shown) or augment IFN- -induction in conjunction with Riplet (Fig. 2*E*). Because RLR-associated molecules naturally reside in cells and facilitate inhibition of low dose viral infection until RLRs become expressed, they may be useful therapeutic targets for an early phase antiviral immunotherapy.

Acknowledgments—We thank Dr. M. Sasai in our laboratory for technical instructions for assay of RIG-I functions and Drs. K. Shimotohno (Keio University), T. Taniguchi (University of Tokyo), and T. Fujita (Kyoto University) for their critical discussions.

REFERENCES

1. Takeuchi, O., and Akira, S. (2008) *Curr. Opin. Immunol.* **20,** 17–22
2. Honda, K., Takaoka, A., and Taniguchi, T. (2006) *Immunity* **25,** 349–360
3. Kato, H., Takeuchi, O., Sato, S., Yoneyama, M., Yamamoto, M., Matsui, K., Uematsu, S., Jung, A., Kawai, T., Ishii, K. J., Yamaguchi, O., Otsu, K., Tsujimura, T., Koh, C. S., Reis e Sousa, C., Matsuura, Y., Fujita, T., and Akira, S. (2006) *Nature* **441,** 101–105
4. Venkataraman, T., Valdes, M., Elsby, R., Kakuta, S., Caceres, G., Saijo, S., Iwakura, Y., and Barber, G. N. (2007) *J. Immunol.* **178,** 6444–6455
5. Yoneyama, M., Kikuchi, M., Matsumoto, K., Imaizumi, T., Miyagishi, M., Taira, K., Foy, E., Loo, Y. M., Gale, M., Jr., Akira, S., Yonehara, S., Kato, A., and Fujita, T. (2005) *J. Immunol.* **175,** 2851–2858
6. Yoneyama, M., Kikuchi, M., Natsukawa, T., Shinobu, N., Imaizumi, T., Miyagishi, M., Taira, K., Akira, S., and Fujita, T. (2004) *Nat. Immunol.* **5,** 730–737
7. Hornung, V., Ellegast, J., Kim, S., Brzozka, K., Jung, A., Kato, H., Poeck, H., Akira, S., Conzelmann, K. K., Schlee, M., Endres, S., and Hartmann, G. (2006) *Science* **314,** 994–997
8. Pichlmair, A., Schulz, O., Tan, C. P., Naslund, T. I., Liljestrom, P., Weber, F., and Reis e Sousa, C. (2006) *Science* **314,** 997–1001
9. Saito, T., Hirai, R., Loo, Y. M., Owen, D., Johnson, C. L., Sinha, S. C., Akira, S., Fujita, T., and Gale, M., Jr. (2007) *Proc. Natl. Acad. Sci. U. S. A.* **104,** 582–587
10. Kawai, T., Takahashi, K., Sato, S., Coban, C., Kumar, H., Kato, H., Ishii, K. J., Takeuchi, O., and Akira, S. (2005) *Nat. Immunol.* **6,** 981–988
11. Meylan, E., Curran, J., Hofmann, K., Moradpour, D., Binder, M., Bartenschlager, R., and Tschopp, J. (2005) *Nature* **437,** 1167–1172
12. Seth, R. B., Sun, L., Ea, C. K., and Chen, Z. J. (2005) *Cell* **122,** 669–682
13. Xu, L. G., Wang, Y. Y., Han, K. J., Li, L. Y., Zhai, Z., and Shu, H. B. (2005) *Mol. Cell* **19,** 727–740
14. Rothenfusser, S., Goutagny, N., DiPerna, G., Gong, M., Monks, B. G., Schoenemeyer, A., Yamamoto, M., Akira, S., and Fitzgerald, K. A. (2005) *J. Immunol.* **175,** 5260–5268
15. Loo, Y. M., Fornek, J., Crochet, N., Bajwa, G., Perwitasari, O., Martinez-Sobrido, L., Akira, S., Gill, M. A., Garcia-Sastre, A., Katze, M. G., and Gale, M., Jr. (2008) *J. Virol.* **82,** 335–345
16. Komuro, A., and Horvath, C. M. (2006) *J. Virol.* **80,** 12332–12342
17. McWhirter, S. M., Tenoever, B. R., and Maniatis, T. (2005) *Cell* **122,** 645–647
18. Saha, S. K., Pietras, E. M., He, J. Q., Kang, J. R., Liu, S. Y., Oganesyan, G., Shahangian, A., Zarnegar, B., Shiba, T. L., Wang, Y., and Cheng, G. (2006) *EMBO J.* **25,** 3257–3263
19. Kayagaki, N., Phung, Q., Chan, S., Chaudhari, R., Quan, C., O'Rourke, K. M., Eby, M., Pietras, E., Cheng, G., Bazan, J. F., Zhang, Z., Arnott, D., and Dixit, V. M. (2007) *Science* **318,** 1628–1632
20. Lin, R., Yang, L., Nakhaei, P., Sun, Q., Sharif-Askari, E., Julkunen, I., and Hiscott, J. (2006) *J. Biol. Chem.* **281,** 2095–2103
21. Zhao, C., Denison, C., Huibregtse, J. M., Gygi, S., and Krug, R. M. (2005) *Proc. Natl. Acad. Sci. U. S. A.* **102,** 10200–10205
22. Arimoto, K., Konishi, H., and Shimotohno, K. (2008) *Mol. Immunol.* **45,** 1078–1084
23. Gack, M. U., Shin, Y. C., Joo, C. H., Urano, T., Liang, C., Sun, L., Takeuchi, O., Akira, S., Chen, Z., Inoue, S., and Jung, J. U. (2007) *Nature* **446,** 916–920
24. Urano, T., Saito, T., Tsukui, T., Fujita, M., Hosoi, T., Muramatsu, M., Ouchi, Y., and Inoue, S. (2002) *Nature* **417,** 871–875
25. Arimoto, K., Takahashi, H., Hishiki, T., Konishi, H., Fujita, T., and Shimotohno, K. (2007) *Proc. Natl. Acad. Sci. U. S. A.* **104,** 7500–7505
26. Sasai, M., Shingai, M., Funami, K., Yoneyama, M., Fujita, T., Matsumoto, M., and Seya, T. (2006) *J. Immunol.* **177,** 8676–8683
27. Douglas, J., Cilliers, D., Coleman, K., Tatton-Brown, K., Barker, K., Bernhard, B., Burn, J., Huson, S., Josifova, D., Lacombe, D., Malik, M., Mansour, S., Reid, E., Cormier-Daire, V., Cole, T., and Rahman, N. (2007) *Nat. Genet.* **39,** 963–965
28. Barral, P. M., Morrison, J. M., Drahos, J., Gupta, P., Sarkar, D., Fisher, P. B., and Racaniello, V. R. (2007) *J. Virol.* **81,** 3677–3684
29. Seol, J. H., Feldman, R. M., Zachariae, W., Shevchenko, A., Correll, C. C., Lyapina, S., Chi, Y., Galova, M., Claypool, J., Sandmeyer, S., Nasmyth, K., Deshaies, R. J., Shevchenko, A., and Deshaies, R. J. (1999) *Genes Dev.* **13,** 1614–1626
30. Pickart, C. M. (2004) *Cell* **116,** 181–190
31. Kim, M. J., Hwang, S. Y., Imaizumi, T., and Yoo, J. Y. (2008) *J. Virol.* **82,** 1474–1483
32. Alexopoulou, L., Holt, A. C., Medzhitov, R., and Flavell, R. A. (2001) *Nature* **413,** 732–738
33. Tanabe, M., Kurita-Taniguchi, M., Takeuchi, K., Takeda, M., Ayata, M., Ogura, H., Matsumoto, M., and Seya, T. (2003) *Biochem. Biophys. Res. Commun.* **311,** 39–48
34. Yoneyama, M., Suhara, W., Fukuhara, Y., Fukuda, M., Nishida, E., and Fujita, T. (1998) *EMBO J.* **17,** 1087–1095

Surg Today (2009) 39:194–200
DOI 10.1007/s00595-008-3826-3

SURGERY TODAY

Original Articles

Innate Immune Therapy with a Bacillus Calmette-Guérin Cell Wall Skeleton After Radical Surgery for Non-Small Cell Lung Cancer: A Case–Control Study

KEN KODAMA[1], MASAHIKO HIGASHIYAMA[1], KOJI TAKAMI[1], KAZUYUKI ODA[1], JIRO OKAMI[1], JUN MAEDA[1], TAKASHI AKAZAWA[2], MISAKO MATSUMOTO[3], TSUKASA SEYA[3], MARIKO WADA[4], and KUMAO TOYOSHIMA[5]

Departments of [1]Thoracic Surgery and [2]Immunology, Osaka Medical Center for Cancer and Cardiovascular Diseases, 1-3-3 Nakamichi, Higashinari-ku, Osaka 537-8511, Japan
[3]Department of Microbiology and Immunology, Hokkaido University Graduate School of Medicine, Sapporo, Japan
[4]Mino Health Center, Mino, Japan
[5]SNP Research Center, RIKEN Yokohama Institute, Yokohama, Japan

Abstract

Purpose. We investigated whether adjuvant immunotherapy with Bacillus Calmette-Guérin (BCG) cell wall skeleton (CWS) and surgical resection was better than resection, with or without other adjuvant therapy, for patients with non-small cell lung cancer (NSCLC).

Methods. The case group comprised 71 patients who underwent radical surgery for NSCLC, followed by BCG-CWS immunotherapy, with follow-up data available. The case–control study was designed with one control selected for each case-group patient. Each control was matched by pathological stage and year of birth (±5 years). BCG-CWS 200 μg was inoculated intracutaneously in the upper arm four times per week (sensitization phase); then at 4-week intervals (therapeutic phase).

Results. The case-group patients received 45 ± 22.6 (average ± SD) cycles of BCG-CWS inoculation. Overall 5-year and 10-year survival rates were 71% and 61% for the case-group patients, and 63% and 43% for the control-group patients. The survival rate of the case group was better than that of the control group (not significant; $P = 0.114$). The same trend was seen in the patients with stage III or N+ NSCLC (not significant; $P = 0.114$, $P = 0.168$). There were no life-threatening adverse events.

Conclusions. BCG-CWS immunotherapy seemed to improve survival after resection of NSCLC, especially locally advanced NSCLC. Moreover, this immunotherapy did not compromise quality of life during treatment.

Key words Bacillus Calmette-Guérin cell wall skeleton · Immunotherapy · Non-small cell lung cancer · Surgical resection · Case–control study

Introduction

The human immune system consists of innate and acquired arms. Recent advances in the field of tumor immunology have revealed two novel findings in these two systems: first, most solid tumors express tumor-associated antigens (TAAs) which are rooted in the aberrance of tumor-related genes;[1] and second, activation of the innate immune system before the acquired system is indispensable for full activation of lymphocyte effectors, or cell-mediated immunity.[2] Considering the former issue, immunotherapy for cancer has been designed with TAA peptides and many cytokines, and this augments lymphocyte-based therapies.[3] Rosenberg et al. challenged clinical trials of a peptide vaccine therapy in which a variety of TAAs were administered to melanoma patients. However, the overall rate of remission (including incomplete remission) was only 2.6%.[4] They used peptide vaccines without adjuvant conjugated, or only with aluminum (non-Toll-like receptor (TLR)-directed adjuvant). These results suggest that innate immunity must be stimulated before the induction of acquired effectors to raise antitumor therapeutic potential.

Microbial components that activate the host innate immune system have been designated as adjuvants. Adjuvants are often used for immunization with pure antigens (Ag) for effective induction of antibody (Ab) production, cytotoxic T cells (CTL), and natural killer (NK) cell activation.[5] Many adjuvants have been identified as ligands for microbial pattern-recognition recep-

Reprint requests to: K. Kodama
Received: January 20, 2008 / Accepted: May 22, 2008

tors such as TLRs.[6] Through sensing microbe patterns, dendritic cells mature to present extrinsic Ag and release lymphocytes from an anergic state.[2,6] The cell-mediated immune system is thereafter activated to target Ag-bearing cells. This concept was demonstrated only recently, and it is now apparent that TLR agonists were being used as popular adjuvants for therapeutic purposes without knowledge of their mechanistic function.

For more than 6 years, clinical trials of many TLR-directed adjuvants have been conducted, aiming at adjuvant-augmented immunotherapy.[6,7] Most of these trials are still in progress with fruitful or anticipated results. Our earlier studies suggested that Bacillus Calmette-Guérin cell wall skeleton (BCG-CWS) has the potential to activate human antigen-presenting dendritic cells and induce interleukin 6 (IL-6), IL-12, tumor necrosis factor alpha (TNF-α),[8] and possibly, CTL.[9] Interferon-gamma (IFN-γ) levels increase in response to BCG-CWS.[10] A sole BCG-CWS without peptides was used in these studies since cancer patients are usually exposed to their own TAAs.[10] Studies on mouse tumor implant models suggest that BCG-CWS induces cross-priming facilitating class I presentation of exogenous antigens.[9] An efficient CTL response against Ag-bearing cells appears evident. These immune responses are attributed to TLR2 and TLR4 in antigen-presenting dendritic cells.[8,11]

The current clinical study was designed to investigate these basic findings on BCG-CWS adjuvant. We anticipated that BCG-CWS alone has the ability to evoke an antitumor immune response because patients with cancer postoperatively still possess TAAs.[10,12] To find out if patients who undergo radical surgery followed by adjuvant BCG-CWS immunotherapy for NSCLC are more likely to have a favorable outcome, we conducted a case–control study.

Materials and Methods

Preparation of BCG-CWS and Its Inoculation Schedule

BCG-CWS, donated by Dr. Azuma,[13] was used as an immunotherapeutic agent in the form of an oil-in-water emulsion, using either mineral oil (Drakeol 6VR) or a metabolizable oil such as squalene or squalane. After sterilizing by heating for 30 min at 60°C, the oil-attached BCG-CWS suspension was inoculated intracutaneously at a final concentration of 1 mg/ml in the upper arm according to the schedule described by Hayashi et al.[12,14] In the sensitization phase, 200 μg was inoculated four times weekly, whereas in the therapeutic phase, the amount inoculated, at 4-week intervals, ranged between 10 and 200 μg, depending on the patient's biological responses, including IFN-γ induction, local skin reaction at the inoculation site, various physical conditions (fever or general malaise), and indicators of laboratory tests showing liver function or inflammatory reactions.

Interferon-γ Induction Test

To evaluate the effect of immunotherapy on BCG-CWS, an IFN-γ induction test was performed at the time of the fourth inoculation in the sensitization phase, and at the time of the first and sixth inoculations in the therapeutic phase. The level of IFN-γ in the peripheral blood was measured before inoculation and 18 h after inoculation. Interferon-γ levels were detected with an enzyme-linked immunosorbent assay at the laboratory of Otsuka Assay (Tokushima, Japan), with the lower limit of sensitivity for detecting human serum IFN-γ being 7.8 pg/ml.

Case–Control Study

In May 1994, the protocol of a pilot study on BCG-CWS immunotherapy for patients with various malignant neoplasms was approved by the Ethical Review Board of Osaka Medical Center for Cancer and Cardiovascular Diseases. At the time of informed consent, we explained to patients about the expected effectiveness and side effects based on previous reports on immunotherapy,[15] chemotherapy,[16] and our survival data of surgery alone. In the 1990s, with the exception of one article published in 1995 from the NSCLC Collaborative Group,[16] there was no clear evidence of the survival benefit of adjuvant chemotherapy for NSCLC.

Written informed consent was obtained from all patients who chose to be treated with immunotherapy, which was started 4–6 weeks after the operation. Among the patients who received BCG-CWS, we recruited 83 NSCLC patients. Between 1994 and 2000, these patients received immunotherapy with BCG-CWS alone as adjuvant therapy after radical surgery for NSCLC. Since the clinical records of 12 patients were unavailable because their operations had been performed at other hospitals, they were excluded from the final analysis. Thus, 71 patients with both clinical records and follow-up data were enrolled in this study as the case group. They did not receive any other adjuvant therapy until recurrence was confirmed.

The case–control study was designed with one control selected for each patient. The control was matched to the patient by pathological stage and year of birth (±5 years). The matched control was recruited from among patients who underwent radical surgery for NSCLC, regardless of adjuvant chemo- and/or radiotherapy, with the shortest interval between the operation from our medical history data file.

Adverse effects of immunotherapy were graded from 0 (none) to 5 (fatal) according to the Common Terminology Criteria for Adverse Events; version 3 (CTCAE) of the National Cancer Institute.

Statistical Analysis

Continuous variables were analyzed by the *t*-test, and categorical variables were evaluated using χ^2 analysis. Overall survival rates and survival rates at each stage were compared between the patients and controls. We performed survival analysis with StatView version 5 (Abacus Computer, Berkeley, CA, USA), and survival curves were calculated with the Kaplan–Meier method.[17] Differences in survival were evaluated with the log-rank test. A P value of less than 0.05 was considered significant.

Results

The case-group patients were inoculated with 45 ± 22.6 (average ± SD) cycles of BCG-CWS over a range of 6–94 cycles (Fig. 1). Table 1 compares the patient characteristics of the case group with the control group. There were no significant differences between the groups in matched criteria, pathological stage (P = 1.000), or histology (P = 0.913). The mean age of the case-group patients was slightly less than that of the control patients (P = 0.087). The male to female ratio of the case-group patients was slightly lower than that of the control patients (P = 0.217). The types of lung resection and the pathological T and N factors were similar in the two groups (P = 0.967, 0.986, and 0.980, respectively). Among 40 control patients with stage II or III disease, 5 had received adjuvant chemo- and/or radiation therapy. The median follow-up was longer than 5 years and was similar in the two groups.

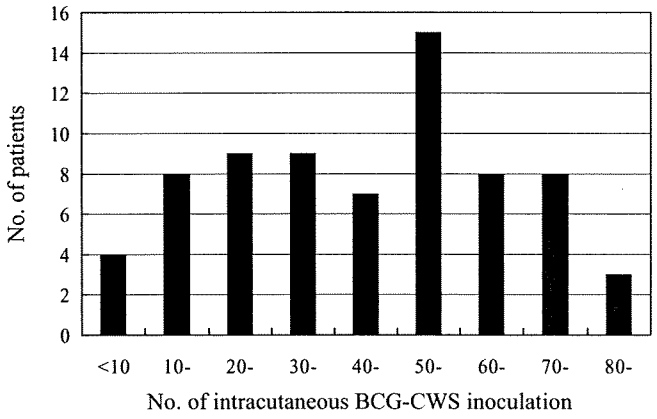

Fig. 1. Postoperative adjuvant immunotherapy with Bacillus Calmette-Guérin cell wall skeleton (*BCG-CWS*) for non-small cell lung cancer. Patient distribution according to the number of treatment courses

Table 1. Case–control study: patient backgrounds

Characteristic	Case patients	Control patients	*P* value
No. of patients	71	71	
Age, years (mean, range)	59 (37–78)	62 (38–78)	0.087
Sex			0.217
Male	43	50	
Female	28	21	
Surgery			0.967
Lesser resection	8	9	
Lobectomy	58	57	
Pneumonectomy	5	5	
Pathological T factor			0.986
T1	36	35	
T2	22	24	
T3	12	11	
T4	1	1	
Pathological N factor			0.980
N0	38	37	
N1	18	19	
N2	15	15	
Pathological stage			1.000
I	31	31	
II	21	21	
III	19	19	
Histology			0.913
Adenocarcinoma	51	49	
Squamous cell carcinoma	16	17	
Large cell carcinoma	4	5	
Median follow-up period (months)	68	66	

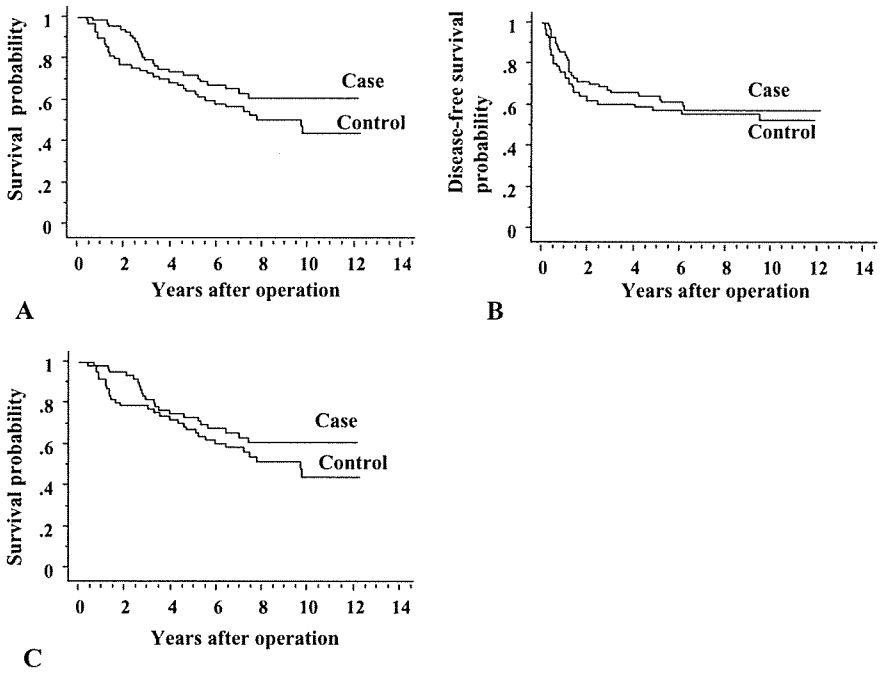

Fig. 2A–C. Kaplan–Meier overall survival estimates. **A** Survival curves. Case-group patients ($n = 71$) versus controls ($n = 71$). $P = 0.114$. **B** Disease-free survival curves. Case-group patients ($n = 71$) versus controls ($n = 71$). $P = 0.473$. **C** Survival curves of 62 gender-matched pairs. Case-group patients ($n = 62$) versus controls ($n = 62$). $P = 0.190$

When patients who had undergone radical surgery for NSCLC hoped to receive adjuvant immunotherapy in spite of a weak IFN-γ induction, the immunotherapy was continued if they had a local skin reaction at the injection site of BCG-CWS, such as an area of erythema greater than 20 mm in diameter, or an induration with an ulcer.[18] As a result, none of the patients given immunotherapy as postoperative adjuvant therapy stopped receiving it. The 5-year and 10-year survival rates were 74% and 62%, respectively, for 20 case-group patients given IFN-γ induction of 35 pg/ml or more, and 70% and 60%, respectively, for 39 given IFN-γ induction of less than 35 pg/ml ($P = 0.700$). The IFN-γ assay was not done for 12 patients.

The overall 5-year and 10-year survival rates were 71% and 61%, respectively, for the case-group patients, and 63% and 43%, respectively, for the control patients group (Fig. 2A). Although the difference was not significant, the survival rate of the case-group patients was better than that of the controls over the observation period ($P = 0.114$). The same trend was observed in disease-free survival between these two groups (Fig. 2B).

To exclude the influence of gender heterogeneity (Table 1) on survival, we selected 62 gender-matched pairs and compared their survival curves. The 5-year and 10-year survival rates were 73% and 61%, respectively, for the 62 case-group patients, and 67% and 44%, respectively, for the 62 control patients ($P = 0.190$; Fig. 2C).

According to the pathological stages, there were no significant differences in survival between the case and control group patients with stage I or II disease (Fig. 3A and 3B). The survival rate of the case-group patients with stage III disease was better than that of the control group patients with stage III disease, although the difference did not reach significance ($P = 0.114$; Fig. 3C). Ten multi-station N2 patients were included in the case group and 8 in the control group. When the survival of pathologically N+ patients was analyzed, both groups showed the same tendency ($P = 0.168$; Fig. 3D).

Table 2. Adverse effects of Bacillus Calmette-Guérin cell wall skeleton treatment

No. of patients	71 (100%)
Nonadverse effect	52 (73)
Adverse effect	19 (27)
Nonmalignant axillary and/or cervical lymph node swelling	9 (13)
ALT and AST elevation (≤grade 2)	6 (8)
Nonmalignant pleural effusion (grade 1)	2 (3)
Infection	1 (1.5)
Neuropathy (grade 2)	1 (1.5)

ALT, alanine aminotransferase; AST, aspartate aminotransferase

Adverse effects were seen in 19 (27%) of the 71 case-group patients (Table 2). These included mild or moderate elevation of alanine aminotransferase and aspartate aminotransferase in six patients, mild nonmalignant pleural effusion in two, and moderate focal infection at the BCG-CWS inoculation site and neuropathy in one patient each. Although there is no grade that refers to the severity of CTCAE, nonmalignant axillary and/or cervical lymph node swelling was observed in nine

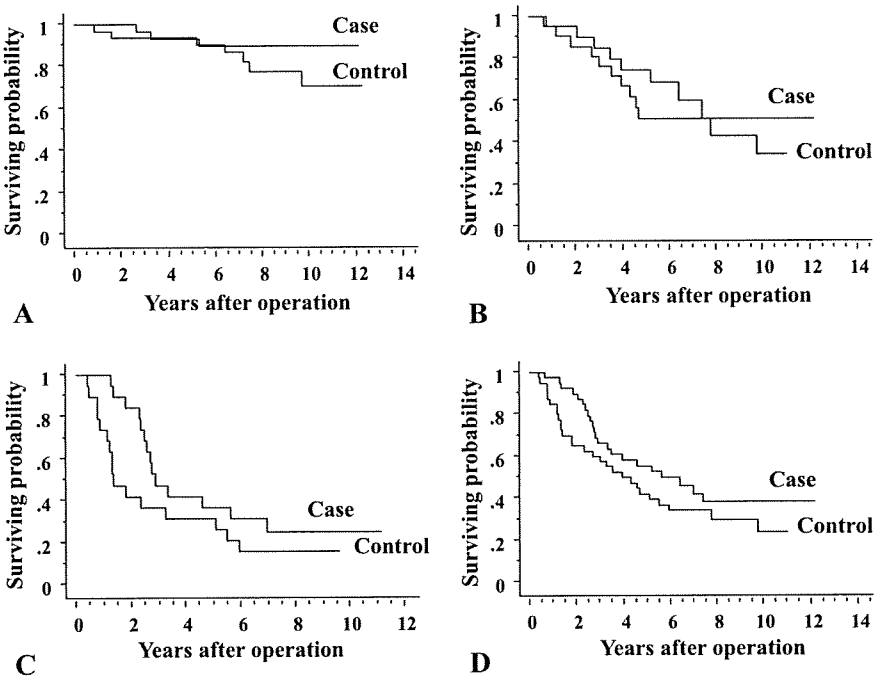

Fig. 3A–D. Kaplan–Meier survival estimates. **A** Stage I. Case-group patients (n = 31) versus controls (n = 31). P = 0.207. **B** Stage II. Case-group patients (n = 21) versus controls (n = 21). P = 0.420. **C** Stage III. Case-group patients (n = 19) versus controls (n = 19). P = 0.114. **D** N(+). Case-group patients (n = 33) versus controls (n = 34). P = 0.168

patients. There was no life-threatening or fatal event. Thirteen of the 19 patients were managed with a temporary dose reduction or discontinuation of BCG-CWS.

Discussion

Immune control of tumor growth can be mediated by the antigen-specific activity of CTLs or by the innate immune response of NK cells. Cytotoxic T cells recognize malignant cells in the context of antigen presentation via major histocompatibility complex (MHC) molecules.[19] Tumor cell recognition by NK cells is antigen-independent and MHC-unrestricted.[20]

Cancer cells share the same MHC as host cells and barely express pathogen-associated molecular patterns (PAMPs). We hypothesized that the inability of tumors to evoke the host immune response is due to the lack of PAMPs in patients with cancer. Supplementation with PAMPs as adjuvants may increase the efficacy of immune responses against tumor antigens (tumor vaccine). Adjuvants are materials added to a vaccine preparation to enhance its immunogenicity. One of the most powerful adjuvants is complete Freund's adjuvant; a suspension of killed mycobacteria in mineral oil. We used BCG-CWS as an adjuvant for this purpose.

Tsuji et al.[8] demonstrated that BCG-CWS can activate immature human dendritic cells (iDC). Antigen presentation and T-cell stimulation are enhanced by BCG-CWS, which also induces up-regulation of the DC maturation marker CD83, and the secretion of inflammatory cytokines such as IL-6, IL-12, and TNF-α. These responses and the increase in antigen-presenting ability indicate that the activation and maturation of DC is induced by CWS-containing mycobacterial peptidoglycan. This suggests that BCG-CWS induces TNF-α secretion from myeloid DC via Toll-like receptor (TLR) 2 and TLR4 and that the secreted TNF-α induces the maturation of DC.

Using a murine subcutaneous and lung metastatic sarcoma treatment model, Mason et al.[21] showed that a local injection of synthetic oligodeoxynucleotides (ODN) containing an unmethylated CpG motif (characteristic of bacterial DNA) could be given with conventional radiation therapy to augment therapeutic efficacy via an apparently immune-mediated mechanism. Combination cancer vaccines with TLR9 agonists such as ODN may induce tumor-specific CD4+ and CD8+ T cells, whose migration and killing activity would be enhanced by radiation therapy. Toll-like receptor expression differences exist between mice and humans; mouse plasmatoid and myeloid DC express TLR9, whereas only human plasmatoid DC does.[22] Mason et al.[21] hypothesized that when radiotherapy is given after TLR agonist injection, the tumor antigens released by dying tumor cells are taken up by activated DC, inducing a tumor-specific T-cell response.

The injection of BCG-CWS sometimes causes lymphadenopathy of the draining lymph nodes (Table 2). We demonstrated the uptake of fluorodeoxyglucose (FDG) into the enlarged lymph nodes not only in the axillary lymph nodes, but also in the cervical and mediastinal lymph nodes by positron emission tomography (PET)

during immunotherapy (data not shown). Lipford et al.[23] reported that among cells within enlarging lymph nodes are many DCs that express increased levels of costimulatory molecules and MHC. Interferon-γ is the final output produced either by the direct stimulation of lymphocytes or by the stimulation of lymphocytes secondary to activation of antigen-presenting cells such as DC. In vitro BCG-CWS induces IL-12 p40 production in peripheral blood culture. Interleukin-12 p40 is an inducible element of IL-12, and in humans may represent IFN-γ-inducing activity.[24]

According to a previous report,[18] BCG-CWS can induce IFN-γ when administered intracutaneously in a patient's upper arm. An elevated serum IFN-γ level is regarded as evidence of a systematic immune response. Interferon-γ is an important immune regulator that performs a wide spectrum of physiologic functions, such as activation of macrophages, NK cells, and CTL, regulation of antigen presentation in many cells, and generation of Type 1 helper T cells (Th1 cells).[25] Our data showed no significant difference in survival between the case-group patients with, and those without IFN-γ induction in the peripheral blood. In this study, we performed IFN-γ assay within 7 months after immunotherapy was started. Matsumoto et al.[24] reported that the levels of production of IFN-γ and IL-10 by lymphocytes were lower in patients with lung cancer than in healthy subjects. In our study, BCG-CWS was repeatedly injected into the skin of both shoulders, for more than 1 year in most patients. When patients receive long-term, repeated inoculations of BCG-CWS, the serum IFN-γ level may increase, especially in those with a good outcome. Our literature search found no report clearly stating an association between increased serum IFN-γ levels and survival benefit in patients receiving BCG-CWS immunotherapy. A recent study of NSCLC patients by Trojan et al.[26] suggested that peritumoral CD8+ T cells exhibit locally higher expression of IFN-γ mRNA; a finding indicative of sustained T-cell reactivity, compared with tumor-infiltrating T lymphocytes (TILs); however, they failed to demonstrate the influence of IFN-γ/CD8 mRNA ratio on overall survival in these patients.

We hypothesized that activation of the innate immune system with BCG-CWS after curative resection for lung cancer may have a survival benefit and conducted a case–control study. Although the difference was not significant, survival of the case-group patients was better than that of the control patients over a long-term follow-up period (Fig. 2). This trend was seen in the subgroups of pathological stage III or lymph node metastasis (Fig. 3C and D). However, there was no difference in survival between the subgroups of p-stage I or II (Fig. 3A and B). These results suggest that monotherapy using BCG-CWS may improve survival without major complications after curative surgery for lung cancer. Patients with advanced lung cancer, especially those with lymph node metastasis, seem to be good candidates for this innate immunotherapy. When patients have micrometastasis to distant lymph nodes, specific cancer antigens may be expressed by the cancer cells and recognized by mature myeloid DC activated with BCG-CWS. The survival benefit of BCG-CWS adjuvant therapy in this series was 17% at 10 years after surgery (Fig. 2A). Tanaka[27] reported a single-institute phase II trial of adjuvant chemotherapy with carboplatin/paclitaxel followed by tegafur and uracil (UFT) for completely resected node-positive (p-stage II-N1 or IIIA-N2) NSCLC. His interim analysis revealed favorable overall and recurrence-free survival of 73% and 49%, respectively, at 3 years, with minimal toxicity. These results suggest that chemotherapy followed by BCG-CWS immunotherapy should be prescribed in a postoperative adjuvant setting after NSCLC resection.

Regarding histological differences between the case and control groups, it was very difficult to completely match three factors at the time of control recruitment. Thus, we gave priority to pathological stage and year of birth. Histology was considered as much as possible but perfectly matched pairing was impossible. According to the survival analysis of BCG-CWS and historical control groups by Yasumoto et al.,[28] all types of lung cancer including squamous cell carcinoma, adenocarcinoma and anaplastic carcinoma were sensitive to treatment with BCG-CWS, and there was no significant difference in survival among those histological types. Their results suggest that the histological differences between case and control group are not of great consequence.

To achieve more effective control of cancer, two modalities should be used with BCG-CWS. The first is the coadministration of a peptide vaccine with BCG-CWS as the adjuvant. The Wilms' tumor gene, *WT1*, is overexpressed in leukemia and a variety of solid tumors, and the WT1 protein has been identified as a tumor-associated antigen.[29] Thus, WT1 products may provide the basis for the development of a new peptide-based anti-cancer immunotherapy. It was demonstrated that 3.0 mg of WT1 therapy can induce a generation of WT1-specific T lymphocytes without damaging normal tissues.[30] Nakajima et al.[31] demonstrated for the first time that a WT1 peptide vaccination combined with BCG-CWS effectively eradicated WT1-expressing tumor cells implanted in mice before vaccination; as a "therapeutic" model, not a "prophylactic" model. Vermorken et al.[32] reported that adjuvant active specific immunotherapy with an autologous tumor cell; namely, BCG (but not CWS) vaccine following surgical resection was more beneficial than resection alone against stage II and III colon cancer. The second modality is the stimulation of NK cells to lyse MHC-unrestricted cancer

cells. A high concentration of IL-10 in the tumor microenvironment may stimulate NK cells to lyse cancer cells, leading to increased availability of tumor-associated antigens and delivery of biologically active molecules, such as heat-shock proteins, needed for the activation of DCs and for effective priming of CTLs against tumor-associated antigens.[33]

We need good manufacturing practices to purify adjuvants such as BCG-CWS for translational research and to coadministrate with more personalized peptide vaccines as a future challenge. In conclusion, our results suggest that BCG-CWS immunotherapy following radical surgery for NSCLC improves overall survival without compromising quality of life.

Acknowledgments. We thank Dr. Ichiro Azuma for kindly providing BCG-CWS. This work was supported in part by a Grant from the Foundation for Promotion of Cancer Research.

References

1. Berinstein NL. Biological therapy of cancer. In: Tannock IF, Hill RP, Bristow RG, Harrington L, editors. Basic science of oncology. New York: McGraw-Hill; 2005. p. 505–39.
2. Iwasaki A, Medzhitov R. Toll-like receptor control of the adaptive immune responses. Nat Immunol 2004;5:987–95.
3. Boon T, Cerottini JC, Van den Eynde B, van der Bruggen P, Van Pel A. Tumor antigens recognized by T lymphocytes. Annu Rev Immunol 1994;12:337–65.
4. Rosenberg SA, Yang JC, Restifo NP. Cancer immunotherapy: moving beyond current vaccines. Nat Med 2004;10:909–15.
5. Seya T, Akazawa T, Uehori J, Matsumoto M, Azuma I, Toyoshima K. Role of Toll-like receptors and their adaptors in adjuvant immunotherapy for cancer. Anticancer Res 2003;23: 4369–76.
6. Kanzler H, Barrat FJ, Hessel EM, Coffman RL. Therapeutic targeting of innate immunity with Toll-like receptor agonists and antagonists. Nat Med 2007;13:552–9.
7. Parkinson T. The future of Toll-like receptor therapeutics. Curr Opin Mol Ther 2008;10:21–31.
8. Tsuji S, Matsumoto M, Takeuchi O, Akira S, Azuma I, Hayashi A, et al. Maturation of human dendritic cells by cell wall skeleton of Mycobacterium bovis bacillus Calmette-Guérin: involvement of Toll-like receptors. Infect Immun 2000;68:6883–90.
9. Akazawa T, Masuda H, Saeki Y, Matsumoto M, Takeda K, Tsujimura K, et al. Adjuvant-mediated tumor regression and tumor-specific cytotoxic response are impaired in MyD88-deficient mice. Cancer Res 2004;64:757–64.
10. Hayashi A, Noda A. Does the cell wall skeleton from Bacille Calmette-Guérin directly induce interferon-gamma, independent of interleukin-12? Jpn J Clin Oncol 1996;26:124–7.
11. Uehori J, Matsumoto M, Tsuji S, Akazawa T, Takeuchi O, Akira S, et al. Simultaneous blocking of human Toll-like receptors 2 and 4 suppresses myeloid dendritic cell activation induced by Mycobacterium bovis bacillus Calmette-Guérin peptidoglycan. Infect Immun 2003;71:4238–49.
12. Hayashi A, Doi O, Azuma I, Toyoshima K. Immuno-friendly use of BCG-cell-wall skeleton remarkably improves the survival rate of various cancer patients. Proc Japan Acad 1998;74:50–5.
13. Azuma I, Kishimoto S, Yamamura Y, Petit JF. Adjuvancity of mycobacterial cell wall. Jpn J Microbiol 1971;15:193–7.
14. Hayashi A, Nakamura H, Sugihara T, Azuma I. BCG-cell wall skeleton completely cures the immunologically eligible acute leukemia patients. Proc Japan Acad 1999;75:295–300.
15. Ochiai T, Sato H, Hayashi R, Asano T, Sato H, Yamamura Y. Postoperative adjuvant immunotherapy of gastric cancer with BCG-CWS wall skeleton. 3- to 6-year follow-up of a randomized clinical trial. Cancer Immunol Immunother 1983;14:167–71.
16. Non-Small Cell Lung Cancer Collaborate Group. Chemotherapy in non-small cell lung cancer: a meta-analysis using updated data on individual patients from 52 randomized clinical trials. BMJ 1995;311:899–909.
17. Kaplan EL, Meier P. Nonparametric estimation from incomplete observation. J Am Sat Assoc 1958;53:457–81.
18. Hayashi A. Interferon-γ as a marker for the effective cancer immunotherapy with BCG-cell wall skeleton. Proc Japan Acad 1994;70:205–9.
19. Boon T, Cerottini J-C, Van Der Bruggen P, Van Pel A. Tumor antigens recognized by T lymphocytes. Annu Rev Immunol 1994;12:337–65.
20. Barao I, Ascensao JL. Human natural killer cells. Arch Immunol Ther Exp 1998;46:213–29.
21. Mason KA, Ariga H, Neal R, Valdecanas D, Hunter N, Krieg AM, et al. Targeting Toll-like receptor 9 with CpG oligodeoxynucleotides enhances tumor response to fractionated radiotherapy. Clin Cancer Res 2005;11:361–9.
22. Koski GK, Czerniecki BJ. Combining innate immunity with radiation therapy for cancer treatment. Clin Cancer Res 2005;11: 7–11.
23. Lipford GB, Sparwasser T, Zimmermann S, Heeg K, Wagner H. CpG-DNA-mediated transient lymphadenopathy is associated with a state of Th1 predisposition to antigen-driven responses. J Immunol 2000;165:1228–35.
24. Matsumoto M, Seya T, Kikkawa S, Tsuji S, Shida K, Nomura M, et al. Interferon gamma-producing ability in blood lymphocytes of patients with lung cancer through activation of the innate immune system by BCG cell wall skeleton. Int Immunol 2001;1: 1559–69.
25. Paul WE, Seder RA. Lymphocyte responses and cytokines. Cell 1994;76:241–51.
26. Trojan A, Urosevic M, Dummer R, Giger R, Weder W, Stahel RA. Immune activation status of CD8+ T cells infiltrating non-small cell lung cancer. Lung Cancer 2004;44:143–7.
27. Tanaka F. UFT (tegafur and uracil) as postoperative adjuvant chemotherapy for solid tumors (carcinoma of the lung, stomach, colon/rectum, and breast): clinical evidence, mechanism of action, and future direction. Surg Today 2007;37:923–43.
28. Yasumoto K, Manabe H, Yanagawa E, Nagano N, Ueda H, Hirota N, et al. Nonspecific adjuvant immunotherapy of lung cancer with cell wall skeleton of *Mycobacterium bovis* Bacillus Calmette-Guérin. Cancer Res 1979;39:3262–7.
29. Cull KM, Glaser T, Ito CY, Buckler AJ, Pelletier J, Halber DA, et al. Isolation and characterization of a zinc finger polypeptide gene at the human chromosome 11 Wilms' tumor locus. Cell 1990;60:509–20.
30. Morita S, Oka Y, Tsuboi A, Kawakami M, Maruno M, Izumoto S, et al. A phase I/II trial of a WT1 (Wilms' tumor gene) peptide vaccine in patients with solid malignancy: safety assessment based on the phase I data. Jpn J Clin Oncol 2006;36:231–6.
31. Nakajima H, Kawasaki K, Oka Y, Tsuboi A, Kawakami M, Ikegame K, et al. WT1 peptide vaccination combined with BCG-CWS is more efficient for tumor eradication than WT1 peptide vaccination alone. Cancer Immunol Immunother 2004;53:617–24.
32. Vermorken JB, Claessen MEC, Van Tinteren H, Gall HE, Ezinga R, Meijer S, et al. Active specific immunotherapy for stage II and stage III human colon cancer: a randomized trial. Lancet 1999;353: 345–50.
33. Mocellin S, Mandruzzato S, Bronte V, Lise M, Nitti D. Vaccines for solid tumours. Lancet Oncol 2004;5:681–9.

Tsukasa Seya
Misako Matsumoto
Takashi Ebihara
Hiroyuki Oshiumi

Functional evolution of the TICAM-1 pathway for extrinsic RNA sensing

Authors' address
Tsukasa Seya[1], Misako Matsumoto[1], Takashi Ebihara[1], Hiroyuki Oshiumi[1]
[1]Department of Microbiology and Immunology, Hokkaido University Graduate School of Medicine, Sapporo, Japan.

Correspondence to:
Tsukasa Seya
Department of Microbiology and Immunology
Hokkaido University Graduate School of Medicine
Kita 15, Nishi 7, Kita-ku
Sapporo 060-8638
Japan
Tel.: +81 11 706 5073
Fax: +81 11 706 7866
e-mail: seya-tu@pop.med.hokudai.ac.jp

Acknowledgements
We thank Drs A. Matsuo, T. Tsujita, A. Ishii, M. Shingai, M. Sasai, and K. Funami in our laboratory for their valuable discussions. This work was supported in part by CREST, JST (Japan Science and Technology Corporation), and by Grants-in-Aid from the Ministry of Education, Science, and Culture (Specified Project for Advanced Research) and the Ministry of Health, Labor, and Welfare of Japan, and by the Takeda Science Foundation, Uehara memorial Foundation, Northtec Foundation, Akiyama Foundation and Mitsubishi Foundation. Financial supports by the Sapporo Biocluster 'Bio-S' the Knowledge Cluster Initiative of the MEXT, and the Program of Founding Research Centers for Emerging and Reemerging Infectious Diseases, MEXT are gratefully acknowledged.

Immunological Reviews 2009
Vol. 227: 44–53

Immunological Reviews
0105-2896

Summary: The type I interferon (IFN) is a host defense factor against microbial pathogens in vertebrates. In mammals, retinoic acid-inducible gene I (RIG-I) and melanoma differentiation-associated gene 5 (MDA5) in the cytoplasm are regarded as sensors for double-stranded RNA (dsRNA) and trigger IFN regulatory factor-3 (IRF-3) activation followed by type I IFN induction through the mitochondrial antiviral signaling (MAVS) adapter. This intrinsic pathway appears to link the main protective responses against RNA virus infection in mammals. On the other hand, human Toll-like receptor 3 (TLR3) is localized in the endosomal membrane or cell surface and signals the presence of extrinsic dsRNA. In response to RNA stimulation, TLR3 recruits the Toll-interleukin 1 receptor domain (TIR)-containing adapter molecule 1 (TICAM-1) adapter and induces IRF-3 activation followed by IFN-β promoter activation. Human TLR3 is localized limitedly extent in myeloid dendritic cells, fibroblasts, and epithelial cells. The TICAM-1 and cytoplasmic MAVS pathways converge at the IRF-3-activating kinase in human cells. The reason for the involvement of this extrinsic mode of IFN-inducing pathways in the dsRNA response remains unknown. In fish, two TLRs, i.e. endoplasmic TLR3 and cell surface TLR22, participate in teleost IFN production without the activation of IRF-3. TLR22 is distinct from mammalian TLR3 in terms of cellular localization, ligand selection, and tissue distribution. TLR22 may be a functional substitute for human cell surface TLR3 and may serve as a surveillance molecule for detecting dsRNA virus infection and alerting the immune system for antiviral protection in fish. In this review, we discuss the fundamentals of the extrinsic dsRNA recognition system, which has evolved to induce cellular effectors to cope with dsRNA virus infection across different vertebrate species.

Keywords: *Toll-like receptor, evolution, dsRNA recognition, TICAM-1 (TRIF)*

Introduction

Invading pathogens express specific pattern molecules and are recognized by host pattern recognition receptors (PRRs) (1, 2), representatives of which are Toll-like receptors (TLRs), Nod-like receptors (NLRs), and RNA helicases [retinoic acid-inducible gene I (RIG-I), melanoma differentiation-associated protein 5 (MDA5), etc.]. These receptors signal the presence of microbial patterns in myeloid dendritic cells (mDCs) and thus induce potent activation of the systemic host defense response (3). Recent studies on pattern receptors of

the innate immune system have increased our understanding of how mDCs mature through infection and subsequently orchestrate cellular immunity (4, 5). These molecules also serve as adjuvants for the induction of antigen-specific acquired immunity. TLRs, RIG-I-like helicases (RLHs), and NLRs are major targets for investigating the induction of robust acquired immune responses upon pathogen stimulation. These studies have been conducted using gene-disrupted mice and in *in vitro* human systems.

It has been reported that human cells induce interferon-β (IFN-β) in response to various RNA structures (6, 7). Double-stranded RNA (dsRNA) and its analog polyinosinic–polycytidylic acid (polyI:C) have been identified as potent immune stimulators of viral patterns and are recognized by PRRs. PRRs link cytoplasmic adapter molecules in these mammalian cells. Cytoplasmic RLH and membrane-associated TLRs that induce IFN-α/β involve the mitochondrial antiviral signaling (MAVS) (also known as IPS-1, Cardif, or VISA) or TICAM-1 [Toll-interleukin-1 receptor (IL-1R) (TIR) domain-containing adapter-inducing IFN-β (TRIF)] adapters, respectively, to converge the signal at IRF-3-activating kinases for IFN-β induction (4, 5, 8). IFN-β induction is IRF-3 dependent in mDCs and fibroblasts/epithelial cells (4, 5). By contrast, IFN-α/β is differentially induced in an IRF-7-dependent manner in plasmacytoid DCs (pDCs) (9). This allows activation of the myeloid differentiation factor 88 (MyD88) adapter protein and IKKα [inhibitor of nuclear factor (NF) κB (IκB) kinase α] kinase, which directly activates the IRF-7 transcription factor (10). However, the molecular assembly and mechanism involved in polyI:C-mediated activation of transcription factors still remain unclear in mice and humans.

Some PRRs preferentially recognize nucleic acid structures that are unique to infectious microbes. Type I IFN induction and cytotoxic T-lymphocyte (CTL)/natural killer (NK) cell activation are major outputs for RNA-sensing PRRs in mammalian cells (5, 11). A variety of RNA sensors in the cytoplasm or membranes are engaged in the detection of microbial RNA. These are expressed in a cell-type specific fashion and participate in IFN-α/β production in various cell types. However, the combinations of these receptors that induce cellular immunity still remain undetermined. It is generally accepted that RNA patterns that are exogenously provided or are produced in bystander cells are internalized by mDCs through phagocytosis and are then recognized by endosomal PRRs. By contrast, RNA patterns produced in the cytoplasm of infected cells are directly recognized by PRRs present in the cytoplasm (12). In this review, we adopted an evolutional approach to study TLRs present on the cell membrane and the recognition of the external dsRNA pattern that is specifically formed in other cells during virus replication.

Fish (teleost) have >20 TLRs that include orthologs of human TLRs and other TLRs unique to lower vertebrates living in water (13, 14). Teleost have orthologs of the IFN-inducing genes of mammals and PRRs for microbial pattern recognition. Teleost also have a TICAM-1 ortholog which has no TRAF-binding site but retains the RIP1-binding site (15, 16). Fish may have orthologs of RLH and NLRs. Hence, by comparing the mammalian PRR receptor/adapter system with that of fish, it is possible to examine the development of the innate recognition system during evolution. Molecular evolution by which the mammalian immune system has been established in the current form can be analyzed through the genomic information of vertebrate TLR systems. In this study, we cast insight into the functional properties of fish TLRs and adapters involved in IFN induction.

Recognition of RNA duplexes in vertebrates

Viral replication usually generates dsRNA in the cytoplasm of infected cells and signals to activate antiviral responses. dsRNA, stem-loop structure of RNA, 5′-uncapped triphosphate of RNA, and specific RNA sequences are rapidly recognized by PRRs in the cytoplasm (4, 5, 17), then implicated in host defense (Fig. 1). Many pattern-sensing receptors have been identified in mammals: PKR (dsRNA-dependent protein kinase), Dicer of the short interfering/microRNA system, RLHs including RIG-I, MDA5, and LGP2, and other helicases. These receptors are accompanied by adapters that transduce the dsRNA-sensing signal downstream. Other RNA-sensing molecules such as helicases may also be present in the cytoplasm to join a molecular assembly for foreign RNA detection. The synthesized dsRNAs are incorporated into these molecular complexes to prohibit RNA replication in virus-infected cells.

TLR3 is present in the early endosome and can recognize dsRNA delivered inside the endosomal membrane (18). TLR3 may not have a direct role in capturing dsRNA generated by virus replication in the cytoplasm, but it has an important role in trapping phagocytosed dsRNA (Fig. 2), which is usually wrapped in a membrane that originates from the infected cell (19). In comparison to the direct recognition system of dsRNA in the cytoplasm, this mode of RNA recognition is unique and sophisticated, concerning activation of cellular immunity. As RNA-sensing TLRs and RLH are conserved across vertebrates (20), we hypothesize

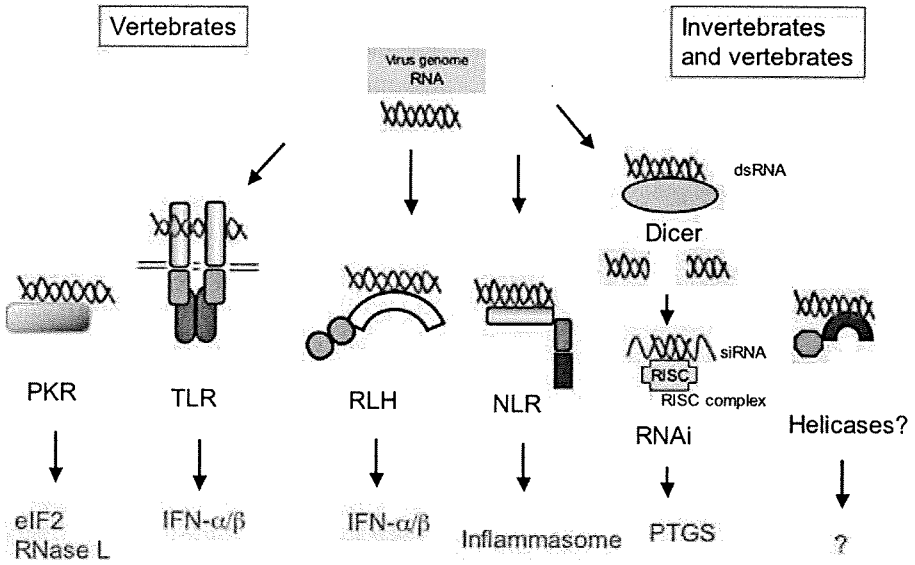

Fig. 1. Various RNA sensors in vertebrates. dsRNA are generated during virus replication. Major RNA sensors in vertebrate cells and their responses on stimulation with dsRNA are indicated. Dicer and RNA-recognizing helicases work even in invertebrates. How dsRNA selects a variety of RNA pattern sensors remains largely unknown. PTGS, post-transcriptional gene silencing.

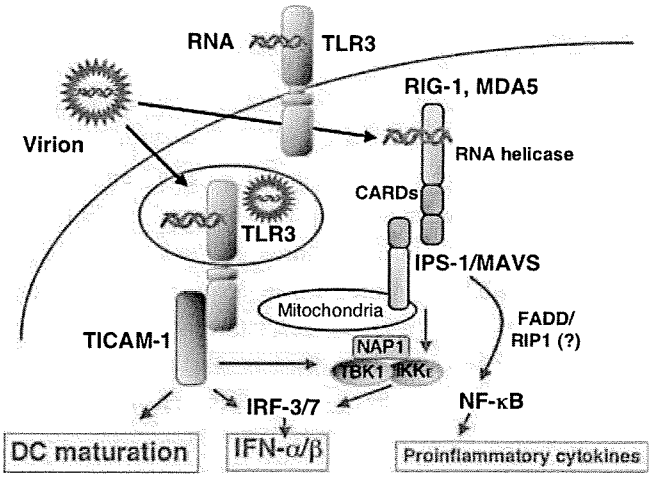

Fig. 2. Cell surface, endosomal and cytoplasmic recognition of dsRNA in mammalian cells. TLR3 is distributed either on the cell surface or in the endosome. Its distribution ratio depends on cell types. RLH (RIG-I and MDA5) reside in the cytoplasm. Adapter molecules, TICAM-1 and MAVS, are localized in the cytoplasm. Upon stimulation, TLR3 recruits TICAM-1 near the endosomal membrane, while MAVS recruits RLH on the mitochondrial membrane. The known outputs of TLR3 and RLH are indicated by red. TLR, Toll-like receptor; RIG, retinoic acid-inducible gene; RLH, RIG-I-like helicase; TICAM, Toll-interleukin 1 receptor domain-containing adapter molecule.

that the two distinct pathways of dsRNA recognition were established in a vertebrate ancestor ~500 Ma and that the two systems have been preserved in mammals (Fig. 2). We focus on the fish membrane-associated dsRNA recognition system and analyze it in terms of its physiological significance and functional feature and also from an evolutionary point of view. We also address the question of why vertebrates need the surface system for dsRNA recognition in addition to the cytoplasmic virus-sensing systems.

Surface recognition of dsRNA in mammals

We initiated a study on the functions of the membrane-associated dsRNA recognition receptor TLR3 in human cells. Stimulation of human fibroblasts/epithelial cells with polyI:C leads to the production of type I IFN. We have produced monoclonal antibodies (mAbs) against human TLR3 and obtained one which blocks polyI:C binding to TLR3, named the mAb TLR3.7 (21). The TLR3.7 mAb interferes with IFN-β production induced by exogenously added polyI:C in human fibroblasts/epithelial cells (18, 21). Hence, it appears that TLR3.7 mAb blocks the interaction between TLR3 and polyI:C on the cell surface by binding to TLR3. If this is the case, human TLR3 must be localized on the cell surface of the fibroblast to capture external dsRNA. This hypothesis was proven by results from fluorescence-assisted cell sorting (FACS) and imaging analyses (Fig. 3A). However, using the same mAb, human mDC TLR3 could not be detected on the surface (18) but was found to be localized in intracellular compartments, particularly endosome (Fig. 3A). mDCs respond to polyI:C to induce type I IFN in the early endosome (22, 23). In this case, how does endosomal TLR3 recognize polyI:C outside the cells? It is rational that there is a transporter that shuttles dsRNA from the cell surface to the endosome in mammals (5). The recognition of dsRNA by TLR3 on the cell surface is

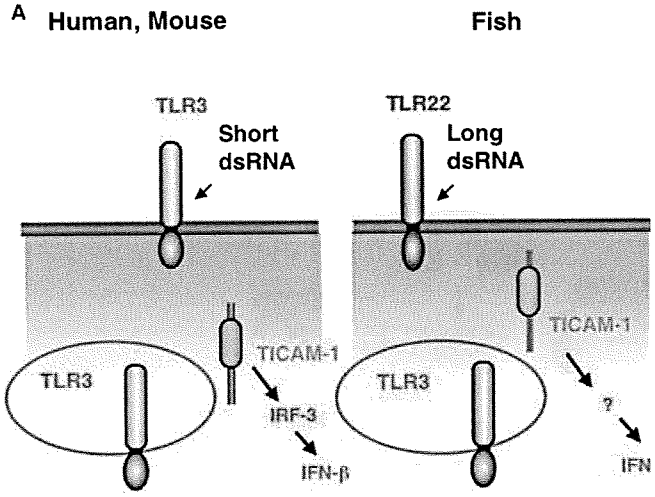

B

IFN-inducing receptors in human and fish

Genes	Human	Fish
TLR3	+	+
RIG-I	+	–
TLR22	–	+
IFN	+	+

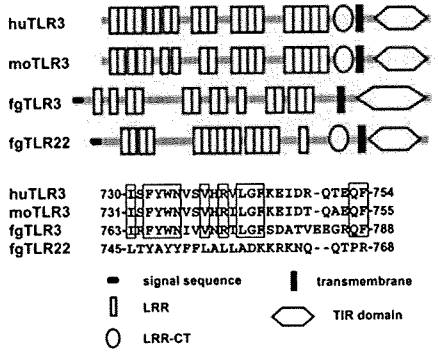

Fig. 3. Different TLRs cover surface dsRNA recognition in fish and mammals. (A) TLR3 and TLR22 in vertebrates. In human and mouse, TLR3 encompasses cell surface and endosomal RNA sensing and induces IRF-3 activation. In fish, two distinct gene products, TLR3 and TLR22, participate in dsRNA sensing. IFN is induced in an IRF-3-independent fashion. Although the structural information is not shown in the panel, mammalian TICAM-1 structurally differs from fish TICAM-1. IRF-3-activating kinase indirectly assembles in an N-terminal portion of mammalian TICAM-1 but not fish TICAM-1. A C-terminal portion contributes to IFN promoter activation in fish cells. (B). Difference of IFN-inducing receptors between human and fish. Upper table indicates that humans lack TLR22 while fish lack RIG-I, although both have IFN-inducible pathways. The structural differences among human (hu) TLR3, mouse (mo) TLR3, fgTLR3, and fgTLR22 are depicted in the lower panel. The primary structures of the linker region (a determinant of TLR3 localization) are shown below the structural models.

experimentally proven by using the mAb probe for determining the localization of human TLR3. However, the dsRNA shuttling system has not yet been proved.

If TLR3 participates in the induction of IFN-β in epithelial cells, its downstream molecules should activate IRF-3. Therefore, we searched for an adapter molecule that could directly interact with TLR3 and activate IRF-3; the molecule was identified by employing the yeast two-hybrid system. It was named TICAM-1 (24) and is now popularly known as TRIF (25).

Human TICAM-1 consists of an N-terminal region (1–234), a TIR domain (235–500), and a C-terminal region (501–680). The N-terminal region of TICAM-1 harbors tumor necrosis factor (TNF) receptor-associated factor (TRAF) family proteins (26, 27) and forms a complex containing IRF-3-activating kinases (28, 29). This kinase complex is crucial for activating the IFN-β promoter (28, 29) and inducing the activation of NK (5, 30) and CTL (12, 31) effector cells (Fig. 4). The C-terminal region of TICAM-1 can recruit receptor-interacting protein-1 (RIP-1), and this event is followed by the activation of other effectors (32). All these signaling events constitute the TICAM-1 pathway. Human and mouse TICAM-1 pathways involve mDC maturation, cytokine/chemokine induction, cross-presentation of exogenous antigens for proliferation of $CD8^+$ T cells (5, 12, 31, 33), NK cell activation (30, 34), and induction of autophagy and apoptosis (35). CD4+ regulatory T (Treg) cells and Th17 cells may be induced by mDCs matured through TICAM-1 signaling. TICAM-1 may act as a platform that recruits various signaling molecules for mDC output in mammals. However, one question that remains unanswered is whether the TICAM-1 pathway is conserved in lower vertebrates such as fish.

Surface recognition of dsRNA in fish

Fish [*Takifugu rubripes* (fg)] have ~20 TLRs and three TLR adapters, i.e. fgMyD88, fgTICAM-1, and fgTIRAP/Mal (36). By using the yeast two-hybrid analysis system, we found at least two TLRs that share the fgTICAM-1 adapter (37). The first report on fgTLRs (13) showed that fgTLR3 and fgTLR22 choose the fgTICAM-1 adapter in fish cells and induce fish type I IFN by recognizing dsRNA. fgTLR3 and fgTLR22 are quite different in their primary structures (Fig. 3B) and are classified into different clades by gene tree analysis (13, 37). However, both fgTLR3 and fgTLR22 directly bind to fgTICAM-1 in fish cells as well as in yeast. Confocal analysis has shown that fgTLR3 resides in the endoplasmic reticulum (ER) and recognizes relatively short dsRNA, whereas fgTLR22 recognizes long dsRNA present on the cell surface (37). The

properties of fgTLR3 and fgTLR22 are summarized in Fig. 3B. fgTLR22 is particular, as fgTLR22 preferentially recognizes long dsRNA, localizes exclusively to the cell surface, and is widely distributed across tissue/organs. In summary, two of the receptors that recognize dsRNA are also involved in the TICAM-1 pathway in fish. The fish TICAM-1 pathway leads to the activation of the IFN promoter.

The next question is how TICAM-1 is assembled by TLR22 to transmit the dsRNA recognition signal. Possible answers may lie in the structural difference between mammalian and teleost TICAM-1 (Fig. 3B). Over-expression of zebrafish (zf)TICAM-1 activates the zfIFN promoter, but zfTICAM-1 does not interact with zfTRAF6 (16). Results from genomic retrieval analysis suggest that zebrafish lacks IRF-3. The zfTICAM-1 N-terminal region does not contain the TRAF6-binding motif (that participates in IRF-3 activation), and the C-terminal region of zfTICAM-1 can adequately activate the zfIFN promoter. This observation suggests the involvement of RIP1-mediated NF-κB activation in zfIFN promoter activation (16, 37).

Human TICAM-1 stimulates IRF-3-mediated type I IFN induction by means of its N-terminal region (38, 39) (Fig. 4). Thus, fish TICAM-1 behaves like human TICAM-1; however, fish TICAM-1 does not employ IRF-3 to activate the IFN-β promoter (16, 40). Although the TICAM-1 pathway is conserved across both fish and humans, the molecular bases for IFN induction in response to extrinsic dsRNA differ in the two vertebrate species (Fig. 3). Our speculation is that although fish cells have an IFN output similar to that of human cells, the signal cascade that leads to IFN production is modally different. Teleost TICAM-1, which is structurally dissimilar to human TICAM-1 (36), might help in explaining the differential selection of the signal pathways.

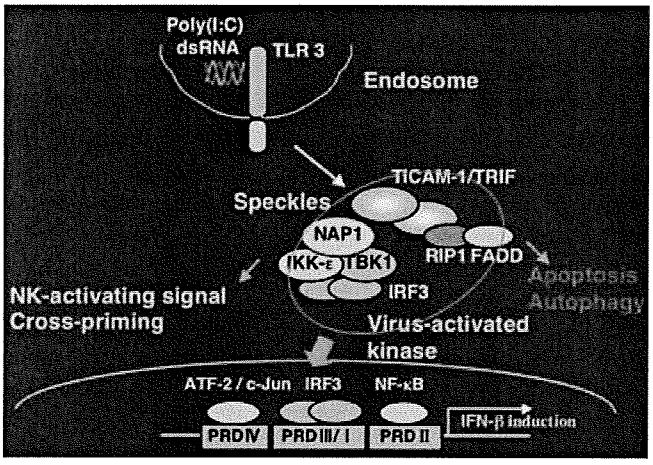

Fig. 4. TICAM-1 is dissociated from TLR3 to form a signaling unit, Speckle. In human cells, TICAM-1 once detached from TLR3 serves as a signaling platform to induce apoptosis, autophagy, NK activation, and cross-priming. TICAM-1 undergoes some modification secondary to complex formation with TLR3 and dissociated from TLR3 with unknown mechanism. The pathways for NK activation, CTL induction, and autophagy are not yet identified, although the pathway for apoptosis is getting clarified. It is undetermined whether surface-expressed TLR3 or TLR22 retain the cellular responses.

How does human TLR3 substitute for TLR22 in mammals?

The differences between TLR22 and TLR3 can be summarized as follows. Based on confocal microscopy and FACS analyses, over-expressed fgTLR22 is localized on the cell surface, while fgTLR3 resides in the ER and endosomes in fish cells (37). fgTLR22 is ubiquitously distributed over the organs/tissues of teleost, while human and fgTLR3 are present only in a limited cell repertoire. These two TLRs do not merge with each other or with fgTICAM-1 in resting cells. When stimulated with polyI:C, a part of the fgTLR22 population enters the cytoplasmic region to merge with fgTICAM-1 (37). Similarly upon stimulation, fgTLR3 is clustered and merges with fgTICAM-1 in the cytoplasm (37). Immunoprecipitation studies have supported their molecular interactions: fgTICAM-1 coprecipitates with fgTLR22 or fgTLR3 in human HEK293 cells. A reporter assay has shown that the dominant-negative form of fgTICAM-1 blocks the fgTLR22- and fgTLR3-mediated IFN promoter activation induced by endogenous fgTICAM-1 in RTG-2 (rainbow trout) cells. Thus, fish have a novel TICAM-1-coupling TLR, TLR22, which is clustered on the cell surface. Although mammals have lost TLR22, TLR3 is distributed on the surface membrane as well as in the endosomes only in some kinds of epithelial cells (41–44), and this appears as though TLR3 compensates for the loss of TLR22 in limited cell types.

We tested the physiological function of fgTLR22 and found that fgTLR22-expressing RTG-2 (rainbow trout) cells become resistant to virus infection (37). We used birnavirus, which is a representative dsRNA virus found in water. Cytopathic effect formation was observed in control cells that did not express fgTLR22, whereas it was barely detected in cells expressing fgTLR22. The level of TCID50 in the supernatant, which reflects virus replication in the cells, was high in the control cells and ~100-fold lower in fgTLR22-expressing cells. Virus RNA levels were suppressed in fgTLR22-expressing cells. Conversely, IFN mRNA was upregulated in virus-infected cells.

In humans, TLR3 is expressed in the endosomes and on the surface of epithelial cells/fibroblasts (18, 22). Expression of TLR3 on the cell surface membrane of human bronchial, bile-duct, and intestinal epithelial cells has also been reported

